

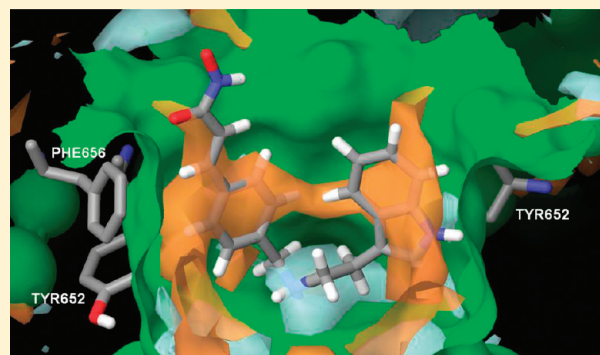
Optimization of the in Vitro Cardiac Safety of Hydroxamate-Based Histone Deacetylase Inhibitors

Michael D. Shultz,* Xueying Cao, Christine H. Chen, Young Shin Cho, Nicole R. Davis,[†] Joe Eckman, Jianmei Fan, Alex Fekete, Brant Firestone, Julie Flynn,[‡] Jack Green, Joseph D. Growney, Mats Holmqvist, Meier Hsu,[§] Daniel Jansson, Lei Jiang, Paul Kwon, Gang Liu, Franco Lombardo, Qiang Lu,^{||} Dyuti Majumdar, Christopher Meta, Lawrence Perez, Minying Pu, Tim Ramsey, Stacy Remiszewski, Suzanne Skolnik, Martin Traebert, Laszlo Urban, Vinita Uttamsingh,[⊥] Ping Wang, Steven Whitebread, Lewis Whitehead, Yan Yan-Neale, Yung-Mae Yao, Liping Zhou, and Peter Atadja

Novartis Institutes for Biomedical Research, Inc., 250 Massachusetts Avenue, Cambridge, Massachusetts 02139, United States

S Supporting Information

ABSTRACT: Histone deacetylase (HDAC) inhibitors have shown promise in treating various forms of cancer. However, many HDAC inhibitors from diverse structural classes have been associated with QT prolongation in humans. Inhibition of the human ether a-go-go related gene (hERG) channel has been associated with QT prolongation and fatal arrhythmias. To determine if the observed cardiac effects of HDAC inhibitors in humans is due to hERG blockade, a highly potent HDAC inhibitor devoid of hERG activity was required. Starting with dacinostat (LAQ824), a highly potent HDAC inhibitor, we explored the SAR to determine the pharmacophores required for HDAC and hERG inhibition. We disclose here the results of these efforts where a high degree of pharmacophore homology between these two targets was discovered. This similarity prevented traditional strategies for mitigating hERG binding/modulation from being successful and novel approaches for reducing hERG inhibition were required. Using a hERG homology model, two compounds, **11r** and **25i**, were discovered to be highly efficacious with weak affinity for the hERG and other ion channels.



INTRODUCTION

The post-translational modification of proteins via acetylation and deacetylation is a powerful mechanism of regulating protein function, stability, activity, and subcellular localization.^{1–12} In cancer and other diseases, enzymes that control posttranslational modifications have altered levels of activity due to genetic and epigenetic changes that accrue on a cellular level. One such mechanism of posttranslational modification is the acetylation of the terminal amino group on lysine side chains, catalyzed by histone acetyl transferases and the deacetylation step that is catalyzed by a family of enzymes known as histone deacetylases (HDACs).¹³ Pharmacological inhibition of HDACs has been shown to be a successful strategy to treat certain forms of cancer, as evidenced by their approved use by regulatory agencies.^{14,15} In addition to their promise as antineoplastic agents, HDAC inhibitors are under extensive study to treat a wide range of disorders including Huntington's disease, fibrosis, cardiac hypertrophy, multiple sclerosis, spinal muscle atrophy, and as anti-infective agents.^{16–23} Several HDAC inhibitors have entered clinical development as anticancer treatments and studies with these and other agents toward nononcology indications are gaining momentum. The two most prominent classes of HDAC inhibitors are

hydroxamates such as vorinostat **1** (SAHA),²⁴ belinostat **2** (PXD-101),²⁵ dacinostat **3** (LAQ824),²⁶ **4** (SB-939),²⁷ and benzamides such as mocetinostat **5** (MGCD-0103)²⁸ and entinostat **6** (SNDX-275 formerly MS-275),²⁹ while Romidepsin (FK228),^{24,30,31} a natural product not belonging to either class, has also received approval from regulatory agencies (Figure 1). There have been several excellent reviews detailing additional compounds undergoing clinical investigation in this highly competitive field.^{32–40} Although these agents hold great promise for a variety of indications, there has been concern about dose limiting toxicities observed in human trials including fatigue, thrombocytopenia, gastrointestinal toxicity, and QT prolongation.^{41–43} Episodes of QT prolongation have been reported for **2**, **3**, **4**, romidepsin, givinostat, and JNJ-26481585, while atrial fibrillation and pericarditis were observed with CHR-3996 and **5**, respectively.²⁸ Because of the wide variety of chemical classes where QT prolongation, ventricular fibrillation, and/or other cardiac toxicities have been reported, there is speculation that the

Received: April 1, 2011

Published: June 08, 2011

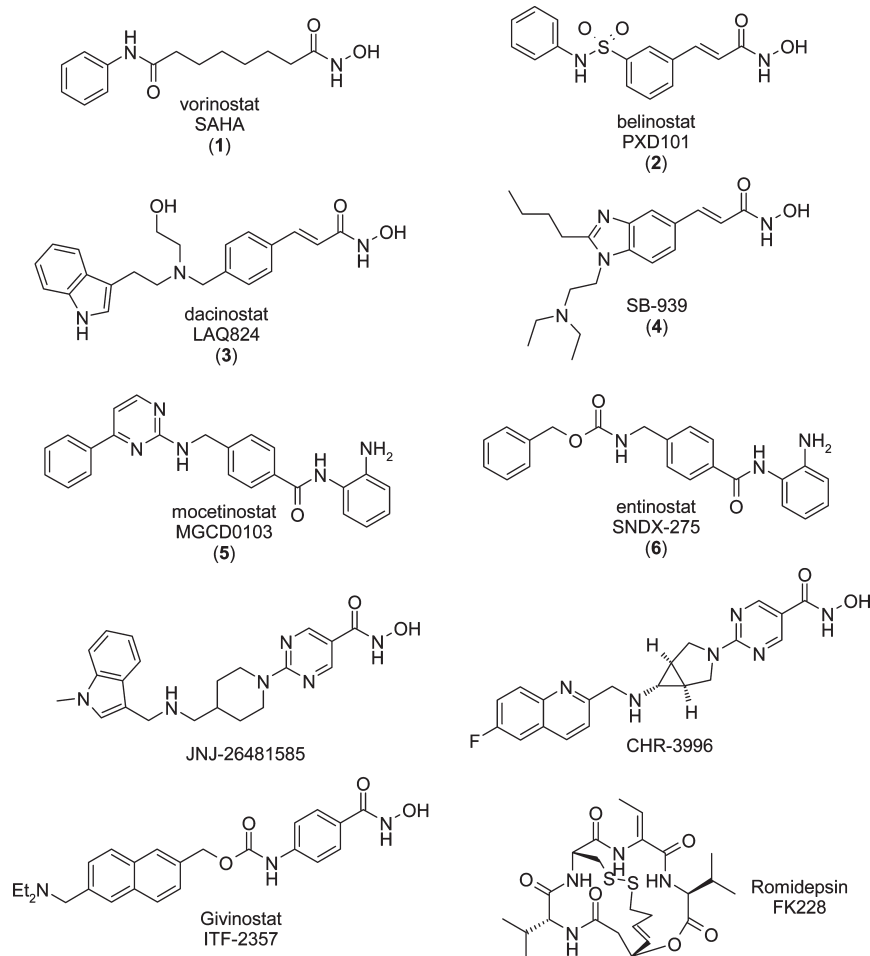


Figure 1. Select clinical and FDA approved HDAC inhibitors.

cardiovascular events are an on-target effect, but this hypothesis had not yet been proven experimentally.^{44–46}

Of the HDAC inhibitors to enter late stage clinical trials, **3** has the greatest in vitro potency against multiple HDAC isoforms as well as the hERG ion channel.^{47–52} Following a number of drug withdrawals from the market due to QT prolongation, torsade de pointes, and sudden death, the hERG channel has become linked with QT prolongation.^{53–57} As part of our effort to develop a second-generation HDAC inhibitor, we initiated a program with the goal of enhancing the in vitro potency and in vivo efficacy of a series of hydroxamate based HDAC inhibitors while simultaneously eliminating the interaction with the cardiac ion channels that have been linked to QT prolongation.⁵¹ We hypothesized that a highly potent HDAC inhibitor devoid of activity against the hERG or other ion channels would either provide a superior clinical candidate or help determine if the observed cardiac effects were a consequence of HDAC inhibition. None of the active clinical compounds demonstrated a substantial (>5000 fold) window between HDAC inhibition and hERG inhibition due to their limited HDAC potency and/or solubility. Compound **1**, for which the most data is publicly available, reaches plasma exposures of only 0.96 μM following a 150 mg/kg oral dose in dog and 1.58 μM following an 800 mg oral dose in human, only marginally surpassing cellular IC_{50} values for cells sensitive to **1**.^{58,59} The lack of cardiac findings in the preclinical and clinical telemetry studies of **1** therefore speaks more to the

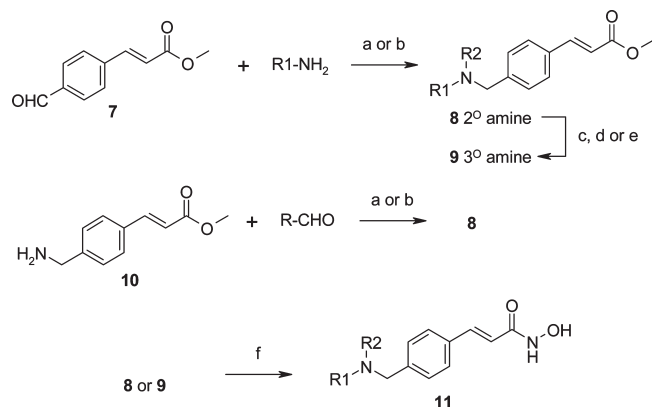
low oral and cardiac exposure with this compound specifically rather than the behavior of HDAC inhibitors in general.⁵⁹ Our efforts were primarily focused at the hERG channel, but advanced compounds were also profiled against sodium and calcium ion channels.⁶⁰ To guide our efforts, we employed homology models of both HDAC-1 and the hERG channel when previously reported approaches to resolve hERG binding were not successful. Herein we report the results of these efforts which led to the identification of several promising compounds including **11r** and **25i**, which demonstrated superior antitumor activity than both **1** and **3**.

CHEMISTRY

The *N*-hydroxy phenylacrylamide scaffold (**2–4**) has been employed extensively by many groups to generate potent HDAC inhibitors and has resulted in at least four clinical programs. This scaffold was further explored by a variety of *N*-alkyl derivatives based on the general structure **11**. Structure-based drug design, physicochemical property modulation, and a matched molecular pair approaches were used in the design of these analogues. Scheme 1 outlines methods where R1-NH_2 , typically a tryptamine or tryptamine analogue, was reacted with methyl 4-formylcinnamate (**7**) via reductive amination to generate substituted methyl 4-aminomethyl cinnamates (**8**). Subsequent alkylation of the secondary amines via reductive amination or reaction with

alkyl halides or epoxides yielded tertiary amines (**9**). Alternatively, when R1 precursors were more readily available as an aldehyde, they were reacted with methyl 4-aminomethylcinnamate (**8**) under similar reductive amination conditions and could be further elaborated as described above. For some compounds,

Scheme 1. General Synthesis of Hydroxamate-Based HDAC Inhibitors^a



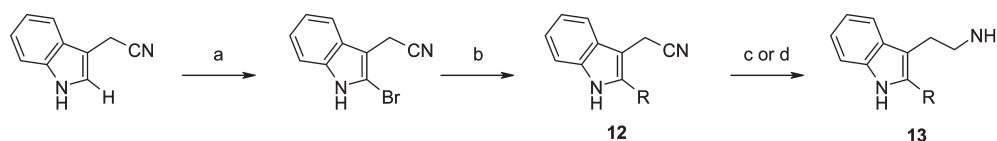
^a Reagents: (a) NaBH(OAc)₃, Et₃N, THF (optional) (method A); (b) SiliaBond cyanoborohydride, (optional); (c) alkyl halide, base; (d) alkyl epoxide, base; (e) aldehyde, method A or SiliaBond cyanoborohydride (f) NH₂OH/H₂O, NaOMe, MeOH (method B).

it was necessary to construct the scaffold using similar reactions but where sequence of the synthetic sequence was altered (e.g., **11r**). Reductive amination with the 2-H indole moiety was not efficient under all circumstances, therefore the 2-methyl indole moiety was optionally used due to higher yields under typical reaction conditions (e.g., the low yielding reductive amination reactions between fluorinated alkyl amines and 1H-indole-3-acetaldehyde was dramatically improved by switching to 2-methyl-indole-3-acetaldehyde). The secondary (**8**) or tertiary amines (**9**) were then converted to the corresponding hydroxamates (**11**) via aqueous hydroxylamine in methanolic sodium methoxide.

The synthesis of 2-heteroaryl indoles was accomplished by *N*-bromosuccinimide mediated bromination of indole-3-acetonitrile followed by Suzuki coupling to form 2-aryl and 2-heteroaryl indoles (**12**). Nitrile hydrogenation was accomplished with rhodium on alumina or borane–THF to yield the modified tryptamine **13** that was used in the synthesis of target compounds (Scheme 2).

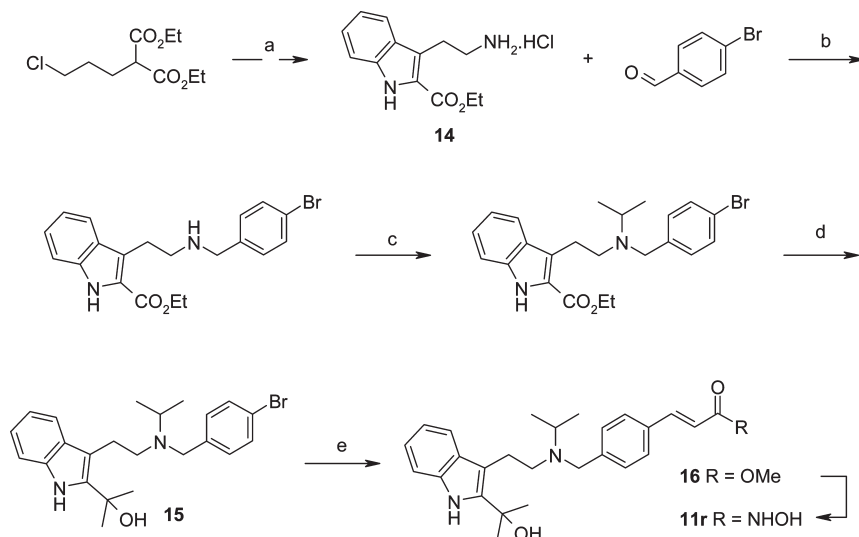
3-(2-Amino-ethyl)-1H-indole-2-carboxylic acid ethyl ester **14** was synthesized using the Japp–Klingemann reaction as previously described (Scheme 3).⁶¹ Reductive amination with 4-bromo benzaldehyde proceeded smoothly using SiliaBond cyanoborohydride. To incorporate the 2-(1H-indol-2-yl)-propan-2-ol motif, several approaches were tried, however under basic conditions, the tryptamine nitrogen formed a lactam with the indole 2-ethyl ester intermediate. The cyclization reaction was prevented by alkylation of the linker nitrogen.

Scheme 2. Synthesis of 2-Substituted Tryptamine Intermediates^a

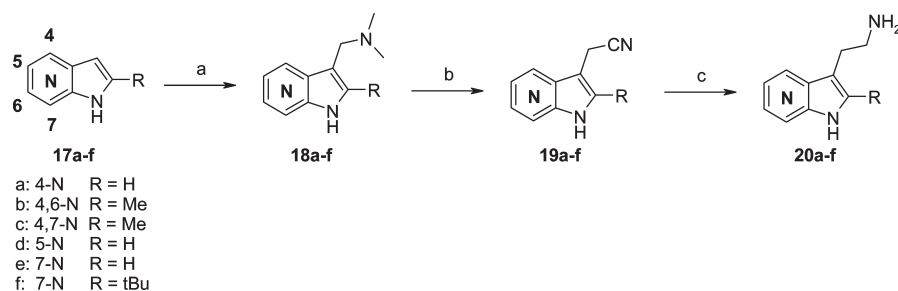


^a Reagents: (a) NBS, DCM (67% yield); (b) Pd(PPh₃)₄, K₂CO₃; (c) H₂ (50 psi), Rh–Al₂O₃, EtOH–NH₄OH (optional) (method C); (d) BH₃–THF (optional) (method D).

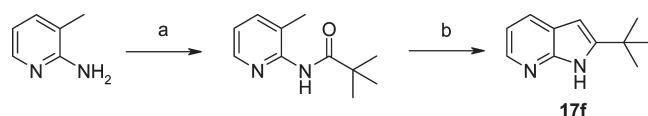
Scheme 3. Synthesis of (E)-N-Hydroxy-3-{4-[(2-[2-(1-hydroxy-1-methyl-ethyl)-1H-indol-3-yl]-ethyl]-isopropyl-amino)-methyl]-phenyl}-acrylamide **11r^a**



^a Reagents: (a) (i) KOH, EtOH; (ii) benzenediazonium; (b) method A; (c) isopropyl iodide, Et₃N, CH₃CN; (d) methyl lithium, THF; (E) methyl acrylate, Pd₂dba₃, 1 equiv H₂O; (f) method B.

Scheme 4. General Synthesis of Azatryptamines^a

^a Reagents: (a) (CH₂O)_m, DMA:butanol, dimethyl amine (method C); (b) (i) MeOSO³Me, THF; (ii) NaCN, H₂O (method D); (c) B₂H₆, BF₃, THF

Scheme 5. Synthesis of 2-*tert*-Butyl-1*H*-indole 17f^a

^a Reagents: (a) (CH₃)₃COCl, K₂CO₃, toluene; (b) *n*-BuLi, THF.

Following *N*-alkylation with isopropyl iodide, methylolithium addition resulted in **15**. A Heck reaction with one equivalent of water yielded **16a**, which was converted to the desired hydroxamate **16b** using aqueous hydroxylamine in methanolic sodium methoxide.

The synthesis of several azaindole derivatives began with functionalization of the 3-position in a straightforward manner via a Mannich reaction (method E) between commercially available azaindoles (**17a–f**) and dimethylamine in the presence of paraformaldehyde. Conversion of **18** to the quaternary ammonium salt followed by a retro-Michael addition reaction with sodium cyanide (method F) resulted in **19** in good yields. Nitrile reduction using rhodium on alumina led to the desired azatryptamine analogues **20** (Scheme 4). Conversion to the desired hydroxamates was accomplished as described in Scheme 1.

Several azaindoles that were not commercially available were synthesized as described below. The synthesis of 2-*tert*-butyl-1*H*-pyrrolo[2,3-*b*]pyridine **17f** (Scheme 5) was accomplished using modifications of previously reported methods. Subsequent elaboration to the azatryptamine **20g** was performed as described above. Reaction of 1-amino pyridinium iodide with a variety of substituted propionic acid ethyl esters provided 2-substituted pyrazolo[1,5-*a*]pyrimidines **21a–c** (Scheme 6). Reduction of the ester with lithium aluminum hydride followed by manganese dioxide oxidation to the aldehyde proceeded in good to excellent yields. Conversion to the nitroethylene **23** was high yielding, however, diborane reduction to azatryptamines **24** were low yielding but scalable, so sufficient quantities of the azatryptamine could be prepared. Elaboration to **25h–25n** proceeded as described in Scheme 1.

RESULTS AND DISCUSSION

The determination of cardiac safety risk with preclinical and clinical compounds has been an area of intense efforts and debate.⁵⁷ Unfortunately, the current standard for assessing the cardiac safety of a particular compound requires information available only after the initiation of clinical development (e.g., unbound concentrations at *C*_{max} in human) or from an integrated risk assessment approach with extremely low throughput (in vivo

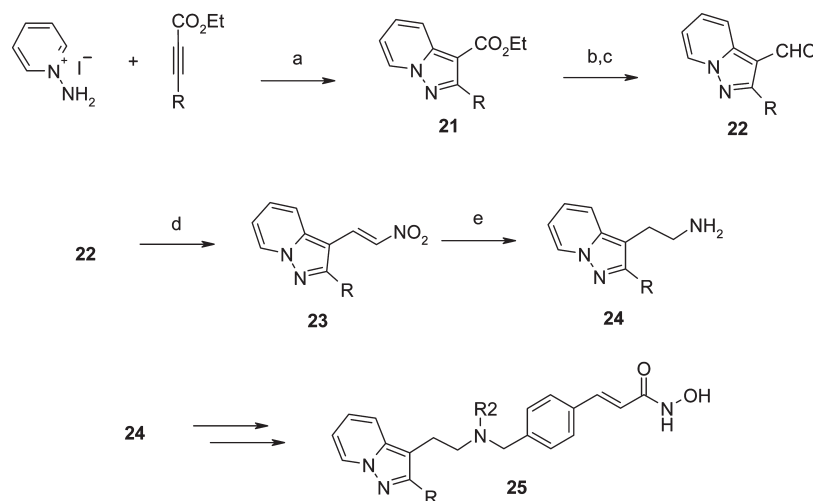
telemetry, measurement of myocardium concentrations, ex vivo cardiac preparations, isolated canine Purkinje fiber, etc.).^{62,63} The accepted definition of the cardiac safety index (CSI) is the ratio of hERG IC₅₀ value (or another measure of adverse cardiac event) and the *C*_{max} of the dose required to generate the desired in vivo effect.⁵⁷ To allow for decision making earlier in the lead optimization process, we introduced an in vitro cardiac safety index (iCSI) parameter defined as the ratio of the hERG IC₅₀, either radioligand binding or the cellular patch clamp, and the cellular IC₅₀ used for compound profiling (antiproliferative activity in the HCT116 cell line). Other levels of inhibition, such as hERG IC₂₀ or a cellular IC₉₀, can be used and may be even more ideal. Similar to other off-target selectivity measurements, this approach helps identify discrete structural modifications that modulate the desired safety window and does not provide false comfort when compounds have weak in vitro activity.

$$\text{CSI} = \frac{\text{hERG IC}_{50}}{C_{\text{max}}(\text{unbound})}$$

$$\text{iCSI} = \frac{\text{hERG IC}_{50}}{\text{cellular IC}_{50}} = \frac{\text{hERG IC}_{50}}{\text{HCT116 IC}_{50}}$$

It has been recommended that, at minimum, the hERG IC₅₀ should be at least 30-fold higher than the free fraction *C*_{max} of a given compound in vivo and a 100-fold margin is generally preferred.⁵⁷ Because it is likely that efficacious concentrations at *C*_{max} will be several orders of magnitude higher than the cellular antiproliferative IC₅₀s, an iCSI goal of 5000 was set to provide sufficient margin of safety prior to the initiation of in vivo studies. In part, this ratio was chosen to be approximately 10-fold higher than the iCSI calculated for **3**. We profiled our compounds against the hERG channel in radioligand binding, manual patch clamp, and automated Q-Patch assays.^{64,65}

hERG activity has been reported to be dependent on several calculable properties including lipophilicity (clogP), amine basicity (p*K*_a), and three-dimensional fit into a pharmacophore model. A large number of HDAC inhibitors from our earlier efforts were screened for hERG activity. For these compounds, the p*K*_as were determined experimentally to determine how well hERG potency correlated with clogP and p*K*_a. Whereas clogP and hERG activity appeared to be only weakly correlated (Supporting Information Figure 1), the basicity of the amine appeared to have some correlation with hERG patch clamp activity (data not shown). The interpretation of clogP SAR is complicated by potential errors in calculation as well as the inherent challenge of modulating this single parameter without affecting other factors known to affect affinity for the hERG

Scheme 6. Synthesis of 2-Substituted Pyrazolo[1,5-*a*]pyridin-3-yl-ethylamine Analogues^a

^a Reagents: (a) K₂CO₃, DMF; (b) LiAlH₄, THF; (c) MnO₂, THF; (d) NH₄OAc, MeNO₂; (e) B₂H₆, BF₃, THF.

channel such as distance between the amine and a hydrophobe, zwitterions, and the introduction of additional substituents such as β -carbonyl, β -hydroxyl, or other moieties that attenuate amine basicity. On the basis of the apparent pK_a correlation and previously reported successes against hERG achieved by modulating amine basicity, we decided to more closely investigate the role the linker amine basicity of **11** played in affecting HDAC and hERG activity. The interpretation of pK_a SAR may not be straightforward due to multiple molecular parameters that are concomitantly altered. To aid our investigation, we made a series of *N*-ethyl and *N*-propyl derivatives (Table 1, compounds **11b–h**) where the hydrogen atoms on the terminal methyl groups were replaced with fluorine atoms in a stepwise manner. The inductive effects of the fluorine atoms decrease the basicity while having negligible effects on the ligand size, flexibility, clogP, or the overall pharmacophore. The amine basicity was thus modulated in relative isolation from other variables that may obfuscate the HDAC and hERG SAR interpretations.

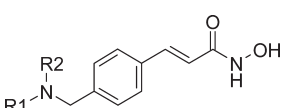
Within analogues of the general formula **11**, an increase in hERG and HDAC binding potency is observed upon conversion to a tertiary amine (Table 1). The ethyl substituent of **11b** increased both the HCT116 cellular and hERG potency nearly 5-fold relative to **11a**. A single fluorine atom on the terminal methyl group (**11c**) had no appreciable effect on HDAC inhibition or hERG affinity. When a difluoromethyl (**11d**) or trifluoromethyl group (**11e**) was incorporated, hERG binding was completely abolished (<5% inhibition at 30 μ M), and there was also a 100–200-fold decrease of HCT116 antiproliferative activity. With two or three fluorine atoms incorporated, the amine basicity is more significantly reduced and thus the equilibrium at physiological pH lies entirely on the side of the neutral amine species. In an attempt to attenuate the inductive effects in a more subtle manner, an additional methylene group was introduced to insulate the amine from the di- and trifluoromethyl groups (**11g** and **11h**). There was also a sharp reduction of both hERG and HDAC inhibition with both of these homologated analogues relative to **11f**. Although it was predicted that the 3,3,3-trifluoropropyl group would adjust the pK_a of **11h** between that of **11c** and **11d**, the measured pK_a s of the ethyl series were higher

than predicted and the measured pK_a s of the propyl series were lower than predicted (Table 1). The modifications at R2 do not significantly affect the measured hydroxamate pK_a (data not shown), therefore all changes in affinity were attributed to the alterations in protonated amine equilibrium. The ammonium ion species distributions in this series was calculated (Figure 2), and only the ethyl and monofluoro analogues (**11b** and **11c**, respectively) were predicted to have any ammonium species present at physiological pH.

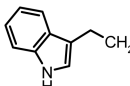
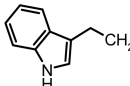
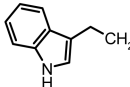
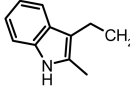
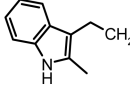
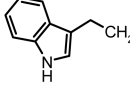
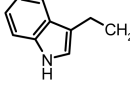
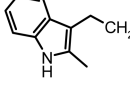
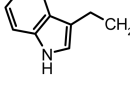
Although correlations between pK_a and hERG binding have been well documented, we are unaware of a similar relationship with regard to HDAC inhibition. To better understand why HDAC inhibition was so highly sensitive to the basicity of the amine linker, an HDAC homology model was analyzed. The docked structure of **11a** places Asp99 and the central amine of this scaffold within 3.4 Å, suggesting an ionic interaction (Figure 3). The dacinostat scaffold (**11**) has demonstrably greater potency than other hydroxamate and benzamide based HDAC inhibitors⁴⁷ that lack a linker with a basic amine. The importance of this interaction is further illustrated when the measured pK_a values were plotted against the HDAC-1 enzymatic and HCT116 cellular IC₅₀ values (Figure 4). The effect of lipophilicity is negligible as a factor in HDAC potency between **11b** and **11e** (Δ clogP = 0.264), however a nearly 200-fold difference in cell growth inhibition is observed. It is interesting to note that when the amine basicity was reduced to effectively eradicate the ammonium species at physiological pH, the antiproliferative activity was indistinguishable from **1**. The correlation between pK_a , hERG, and HDAC inhibition indicates that modulation of amine basicity would be an unsuccessful approach for improving the iCSI within this series.

Another proven approach for reducing hERG activity is the formation of zwitterions by the incorporation of a carboxylic acid or similar motif (e.g., fexofenadine).⁶⁶ The 2-position of the indole ring position was chosen for its ease of substitution and exposure to solvent in our docking models (Figure 3). The HDAC-1 enzymatic potency of **11j** was slightly reduced compared to **11a**, however in several cellular assays, no appreciable activity was observed, presumably due to decreased cellular and nuclear penetration (Table 2). It appeared that incorporation of

Table 1. Inhibitory Activity and iCSI of Compounds against HDAC-1, HCT116, and hERG in Relation to the pK_a of the Linker Amine



11

Compound	R1	R2	IC ₅₀			iCSI	Amine pKa	
			HDAC-1	HCT116	hERG ^a		Predicted	Measured
11a		H	15	30	27,460	915	7.74	7.65
3		CH ₂ CH ₂ OH	15	19	10,300 ^b	542	6.65	7.5
11b		CH ₂ CH ₃	22	7	5,920	846	7.15	nd
11c		CH ₂ CH ₂ F	13	10	5,770	577	5.56	nd
11d		CH ₂ CHF ₂	120	780	4%	>38	4.32	4.65
11e		CH ₂ CF ₃	210	1,370	0%	>22	2.88	3.2
11f		CH ₂ CH ₂ CH ₃	12	6	6,680	1113	7.18	7.9
11g		CH ₂ CH ₂ CHF ₂	130	1,350	0%	>22	5.87	5.8
11h		CH ₂ CH ₂ CF ₃	47	680	2%	>44	5.35	4.75

^a Radioligand binding assay. ^b Manual patch clamp assay.

zwitterions would not be a successful approach, thus alternate approaches were considered.

We next explored discrete structural modifications aimed at exploiting structural differences between the HDAC and hERG proteins and utilized a previously disclosed hERG homology model.⁶⁷ **11a** was docked into this model (Figure 5), and several key interactions appeared to correlate with the hERG SAR in this series. In the hERG homology model, the amine sits in a hydrophilic pocket (gray), while the indole and phenyl rings bind within a hydrophobic belt (brown) in the hERG channel. The HDAC homology model was in agreement with data that the linker amine and the phenyl ring of **11** make key interactions with Asp99 and Phe205, respectively (Figure 3). The indole moiety lies on the surface of the HDAC enzyme but in a hydrophobic pocket when docked into the hERG homology model. We hypothesized that these differences could be used in

our favor with the introduction of amphiphilic modifications. The 2-phenyl indole analogue **11k** improves HCT116 cell growth inhibition by an order of magnitude relative to **11a**, however the iCSI is reduced due to a more dramatic increase in hERG inhibition. The 2-pyridyl analogue **11l** has a lower iCSI than the phenyl analogue **11k**, but the potential to form an internal hydrogen bond between the pyridyl nitrogen and indole NH may have rendered this analogue less polar than first anticipated. The 3-pyridyl 5-methoxy moiety **11m** was designed to force the pyridine ring out of planarity with the indole ring and thus prevent the formation of a similar internal hydrogen bond. The iCSI of this analogue is improved relative to **11k** and **11l**, and we therefore decided to further explore this tactic of utilizing amphiphilicity as a wedge between hERG and HDAC activity.

We next examined 5-membered heterocycles at the indole 2-position, and one of the most potent hERG blockers within this

series was **11n** ($IC_{50} = 480$ nM). Low yielding Suzuki reactions hampered a more thorough exploration at this position, however **11o** demonstrated that bulky, polar substituents at this position could significantly decrease hERG activity. The loss of HDAC activity of **11o** was surprising given the range of steric bulk that had previously been tolerated at this position (e.g., **11m**). **11p** has an improved iCSI relative to **11a**. We wondered if replacing a methyl group of **11p** with a hydroxyl group might provide the best balance of steric bulk while simultaneously introducing some lipophilicity to disfavor binding to the hERG channel. While the direct hydroxy analogue of **11p** was not synthesized, **11r** was tested in a manual patch clamp assay and the IC_{50} in this assay was determined to be >30 μ M (36% inhibition at 30 μ M) while being nearly 5-fold more potent in the HCT116 cell growth inhibition assay than **3**, resulting in an iCSI greater than 7500. By way of a comparison of **11q** and **11a**, we conclude that the reduction in hERG binding was not due to the incorporation of the *N*-isopropyl moiety. Given this evidence that tertiary amines increase hERG channel blockade within this series, **11r** validated the hypothesis of using targeted amphiphilicity to improve the iCSI.

The PK parameters of **11r** in HCT116 tumor bearing nude mice and naïve Sprague–Dawley rats were determined. The

in vivo PK is dominated by a high volume of distribution, rapid extra hepatic clearance, and a short half-life which limits the overall exposure when dosed orally or intravenously. The in vivo PK of **11r** was similar to other compounds in this class that we have examined (data not shown), however the high in vivo clearance was greater than predicted by the stability observed in mouse liver microsomes. To investigate this apparent in vitro/in vivo disconnect further, we examined the plasma stability of **11r**. In mouse plasma, only 54% of the compound remained after three hours of incubation indicating that plasma instability was likely contributing to the rapid clearance. Compound **3**, like other analogues based on scaffold **11**, has low rodent plasma stability but is stable in human plasma, suggesting a species-dependent effect that could overestimate the rate of human clearance. Internal studies demonstrated hydroxamates in this series are stable in thermally denatured mouse plasma. Taken together with recent publications point to enzymatic processing of esters and hydroxamates in rodent plasma, rat PK may be an extremely poor predictor of human PK with this class of compounds.⁶⁸ For these reasons, rodent PK was a less decisive factor in compound progression with this class of compounds.

Because of the low oral exposure in mice, the in vivo efficacy of **11r** was evaluated in the HCT-116 human colon xenograft model using iv administration (Table 3). Following a determination of

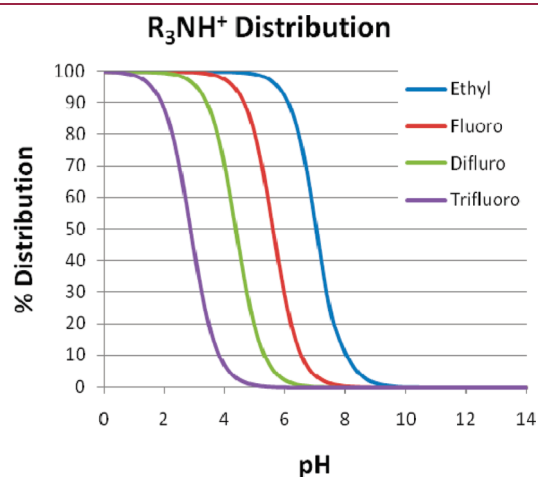


Figure 2. Calculated species distribution plots of tertiary amines **11b–e**. The predicted amount of the protonated amine species is plotted as a function of pH.

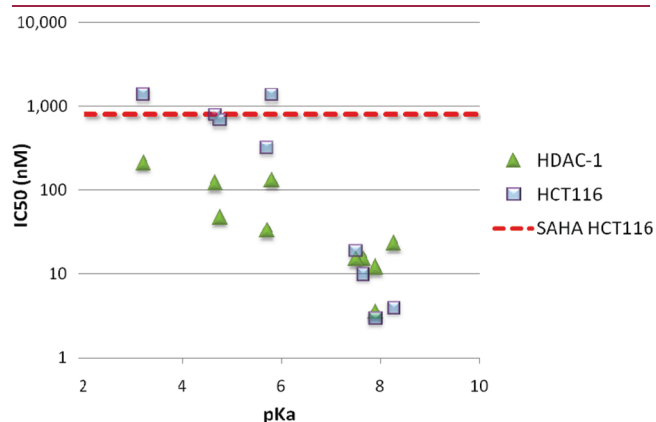


Figure 4. Experimentally determined pK_a versus in vitro activity. Triangles represent activity in the HDAC-1 biochemical assay. Squares represent activity in the HCT116 cellular proliferation assay.

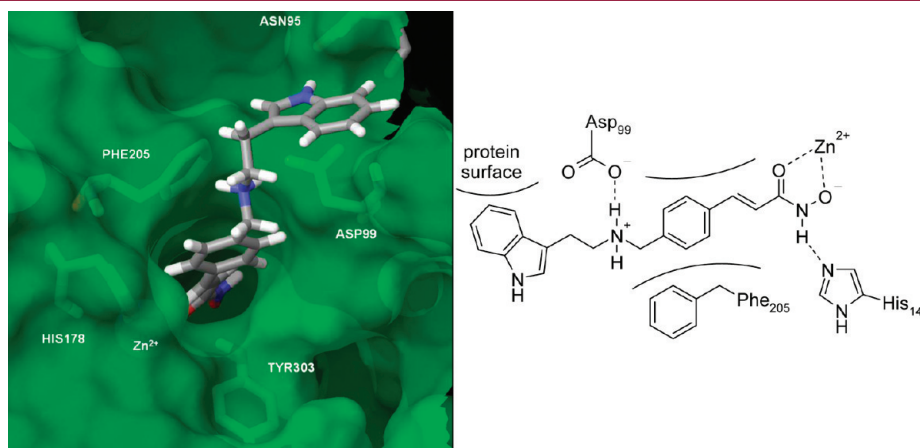


Figure 3. HDAC-1 Homology model with the docked structure of **11a**. Proposed interactions of **25i** and HDAC-1 enzyme based on homology model.

Table 2. Inhibitory Activity and iCSI of Compounds against HDAC-1, HCT116, and hERG

11

Compound	R1	R2	IC ₅₀ (nM)			iCSI
			HDAC-1	HCT116	hERG ^a	
11a		H	15	30	27,460	915
11j		H	23	nd	(6%)	nd
11k		H	12	3	1,480	493
11l		H	12	15	1,540	103
11m		H	1.3	4.6	8,480	1,843
11n		H	49	<1	480	>480
11o		H	17	350	31,240	89
11p		H	2	2	7,450	3,725
11q		CH(CH ₃) ₂	23	6	5,870	978
11r		CH(CH ₃) ₂	4	4	36% ^b	>7,500

^a Radioligand binding assay IC₅₀. ^b Manual patch clamp assay (% inhibition at 30 μM).

the maximum tolerated dose (MTD: defined as the dose that resulted in no deaths and less than 20% body weight loss following 5 days of dosing), animals were treated once daily with **11r** at 10 mg/kg, iv, for a total of 7 days. Results are reported as %T/C, determined by the ratio of the change in tumor volume of treated animals to the change in tumor volume of the control animals, or % regression, determined by the ratio of the change in tumor volumes of the treated animals to the initial volume of the treated group. At this dose, the maximum efficacy observed was 22% tumor regression and mean body weight change of −17.7% (Figure 6). Dosing was discontinued on day 7 due to body weight loss greater than 20% in a subset of animals. The positive control, 5-fluorouracil, administered at 75 mg/kg, iv, resulted in T/C = 43%. Tumor regressions were also observed in the HH human cutaneous T-cell lymphoma (CTCL) xenograft model following once daily treatment with **11r** at 5 mg/kg (data not shown).

Building on the success of amphiphilic modifications, we focused on improving the iCSI by replacing the indole moiety with a more polar heterocycle. A systematic exploration of azaindole analogues of **11a** was initiated where single and double

nitrogen replacements were synthesized. While analogues with nitrogen replacements of C4–C7, either singly or in combination (**25a–e**), resulted in no appreciable hERG inhibition up to 30 μM (Table 4), the HCT116 antiproliferative activity in this series was also diminished to varying degrees. Of these analogues, the 7-azaindole analogue **25e** retained the most HCT116 antiproliferative activity and was explored further. Introduction of a *tert*-butyl group at the 2-position of 7-azaindole ring resulted in **25f** with an iCSI at least 16-fold better than **3**.

For C8 and C9 azaindoles, the imidazo[1,2-*a*]pyridine modification **25g** was not well tolerated but more encouraging results were obtained with the pyrazolo[1,5-*a*]pyrine analogue **25h**. This modification was the only azaindole that increased the HDAC-1 enzymatic and cellular antiproliferative activity with a concomitant reduction of affinity for the hERG ion channel relative to **3**. The SAR was expanded at the 2-position of the pyrazolo[1,5-*a*]pyrine and on the amine nitrogen of the linker. Introduction of a 2-methyl group (**25i**) resulted in an additional 4-fold improvement in cellular activity without an apparent effect on hERG activity, resulting in an iCSI of greater than 6667-fold.

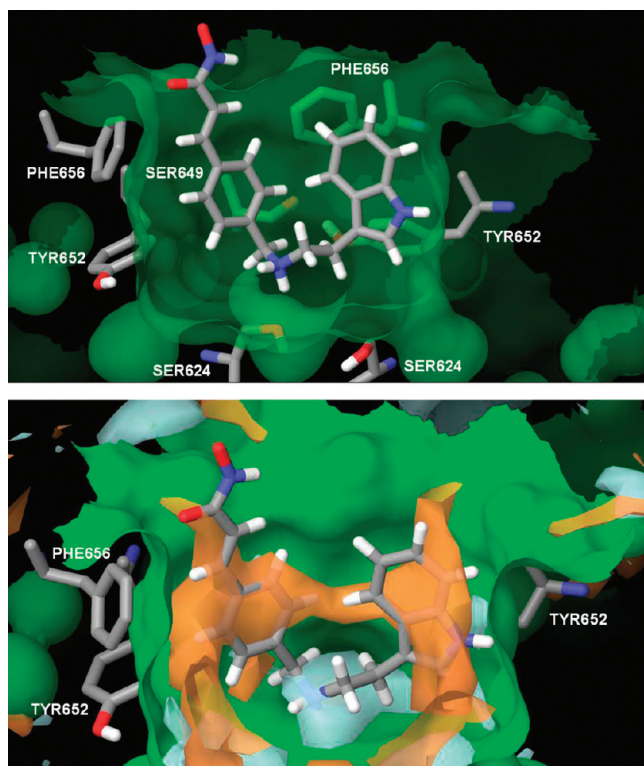


Figure 5. hERG homology models of **11a** with transparent binding surface (top) and binding preferences (bottom). Orange volumes represent areas in which hydrophobic groups are favored, while the light-blue volumes represent regions in which hydrophilic groups are favored.

Table 3. PK Parameters of **11r** in Sprague–Dawley Rats and HCT116 Tumor Bearing Nude Mice

mean PK parameters	rat		mouse	
route	iv	po	iv	po
dose (mg/kg)	5	10	5	20
AUC ($\mu\text{M}\cdot\text{h}$)	1.307	0.336	0.463	0.0653
CL (mL/min/kg)	66		176	
V _{ss} (L/kg)	7		5.9	
T _{1/2} (h)	1.3		1.0	
C _{max} (μM)		0.204		0.056
F %		5		4

Larger hydrophobic groups such as ethyl (**25j**) and phenyl (**25k**) had little effect on cell growth, but in the case of **25k**, apparently re-established the hERG pharmacophore (hERG IC₅₀ = 10.2 μM). Introduction of the isopropyl group on the linker nitrogen resulted in increased affinity for the hERG ion channel, confirming the difficulty of avoiding hERG activity with tertiary amines on this scaffold. It is noteworthy that in each and every case the azaindoles abrogated hERG activity and even facilitated the reintroduction of additional hydrophobic groups with a minimal increase in hERG blockade.

Compounds **25f** and **25i** were selected for more extensive in vitro and in vivo characterization. Compound **25i** has higher intravenous exposure, lower clearance, and a lower volume of distribution than **11r** or **25f** (Table 5). After a single 5 mg/kg intravenous dose, tumor concentrations of **25i** are maintained

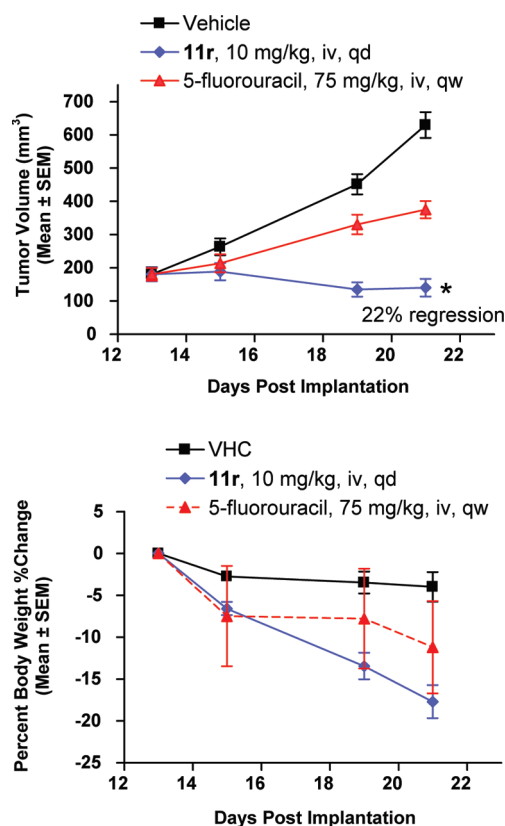


Figure 6. Tumor volumes and body weight changes in the HCT-116 human colon xenograft model in athymic female nude mice following treatment with vehicle, **11r**, or 5-fluorouracil. Treatments were initiated on day 13 post implantation when mean tumor volume reached approximately 180 mm³. **11r** was administered in tartaric acid, iv, qd for 8 total doses. 5-Fluorouracil was administered in 1× phosphate buffered saline as a single dose. Data is expressed as mean ± standard error of the mean (SEM). $p < 0.05$ compared to vehicle controls using a one-way ANOVA.

above the HCT116 LD₅₀ value (4 nM) for 24 h while plasma and tumor concentrations are well below the hERG IC₅₀. Despite high in vivo clearance and low plasma stability, plasma levels of **25i** remained above the cellular LD₅₀ and well below the hERG IC₅₀ (31% inhibition at 30 μM) for 8 h, suggesting the potential for achieving a suitable CSI following oral administration in higher species. Although the plasma exposure of **25f** is slightly higher than **25i** in mice when dosed orally, **25f** could not be quantified in the tumor homogenate. On the basis of excellent solubility (>1 g/L at pH 6.8) and higher tumor exposure, **25i** was selected for in vivo efficacy studies.

The in vivo efficacy of **11r** and **25i** were compared against previous studies of **1** and **3**. Because of poor solubility, we were unable to formulate and dose **1** greater than 150 mg/kg iv. Although others have reported modest efficacy at these doses, we did not observe significant in vivo tumor growth inhibition in our efficacy models at these doses (data not shown). Because **1** had demonstrated clinical efficacy, we chose to compare **11r** and **25i** with the published HCT116 xenograft data from the FDA submission of **1**, where 57% growth inhibition was observed (Figure 7). At 100 mg/kg, iv, **3** resulted in statistically significant tumor growth inhibition with a $T/C = 20\%$. Although **11r** was not tolerated when dosed on a daily schedule for more than one week, significant tumor regressions on a truncated dosing

Table 4. Inhibitory Activity and iCSI of Compounds against HDAC-1, HCT116, and hERG^a of Azaindole Analogues

25

Compound	R1	R2	IC ₅₀ (nM)			iCSI
			HDAC-1	HCT116	hERG ^a	
11a		H	15	30	27,460	915
3		CH ₂ CH ₂ OH	15	19	10,300 ^b	542
25a		H	11	4,180	43%	>7
25b		H	31	172	7%	>174
25c		H	8	1,540	17%	>19
25d		H	21	4,120	0%	>7
25e		H	5	122	20%	>256
25f		H	1.5	3.4	34%	>8,823
25g		H	10	198	8%	>151
25h		H	6	19	26%	>1,579
25i		H	3	4.5	31%	>6,667
25j		H	6	12	27%	>2,500
25k		H	2	3.2	10,400	4,106
25l		CH(CH ₃) ₂	1	1.0	10,030	10,030
25m		CH(CH ₃) ₂	1	0.9	7,520	8,356
25n		CH(CH ₃) ₂	3	1.3	8,160	6,277

^a Radioligand binding assay (% inhibition at 30 μ M). ^b hERG patch clamp assay.

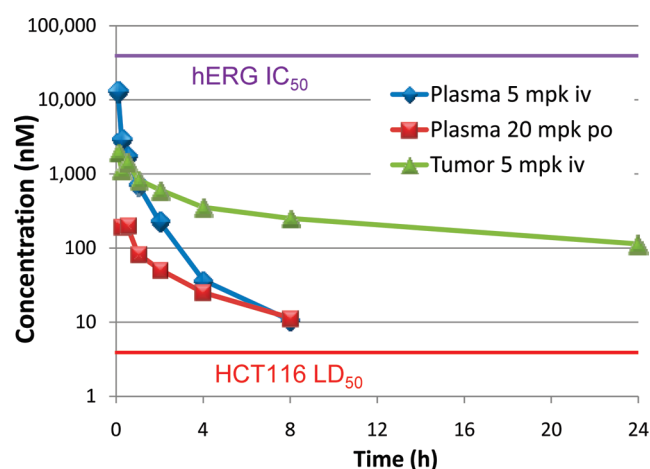
schedule were observed, suggesting that greater in vitro potency in the cellular antiproliferation assays may translate into greater in vivo efficacy with a better tolerated compound.

On a daily intravenous dosing schedule, compound **25i** dosed at 25 or 50 mg/kg resulted in antitumor activity and tumor

regressions, respectively, following 13 days of treatment in the HCT-116 human colon xenograft model (Figure 8). The anti-tumor activity of **25i** corresponded to approximately 15% mean body weight loss at both dose levels. Common dose limiting toxicities of HDAC inhibitors include anorexia, fatigue, body

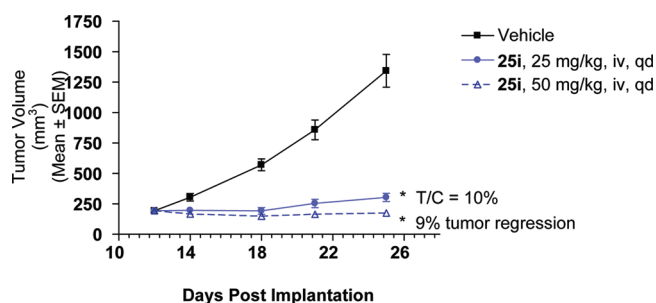
Table 5. PK Parameters of 25i and 25f in Sprague–Dawley Rats and HCT116 Tumor Bearing Nude Mice

mean PK parameters	25i				25f	
	rat		mouse		mouse	
route	iv	po	iv	po	iv	po
dose (mg/kg)	2	10z	5	20	5	20
AUC ($\mu\text{M}\cdot\text{h}$)	2.56		5.10	0.362	2.44	0.474
CL (mL/min/kg)	36.5		46.4		95.0	
V _{ss} (L/kg)	1.99		1.46		4.5	
T _{1/2} (h)	0.915		1.44		3.3	
C _{max} (μM)		0.061		0.202		0.849
F %		nd		2		4

**Figure 7.** Plasma and tumor pharmacokinetics of 25i in HCT116 tumor bearing mice.

weight loss, thrombocytopenia, lethargy, and gastrointestinal effects. In the current studies, the more pronounced efficacy and body weight loss of 11r and 25i may be reflective of the greater HDAC potency of these compounds rather than any generalized toxicity of the compounds per se, however more definitive toxicology studies are warranted to determine if these speculations are accurate (Table 6).

The iCSI of several HDAC inhibitors that are undergoing clinical trials were determined and compared with several compounds in this series. Whereas 3 is the only clinical compound in this set that exhibits activity in the hERG patch clamp assay at concentrations less than 30 μM , the remaining compounds are significantly less potent in the HCT116 proliferation assay, creating a challenge in the assessment of cardiac safety. Because cardiac safety is typically predicted based on ratios of concentrations needed to affect the hERG channel function and those needed for target inhibition, low patch clamp activity does not provide for a complete safety assessment and may lead to unexpected results in more advanced and costly animal models, especially with compounds of relatively low on-target activity or with the potential for high C_{max} levels. Many organizations choose to use hERG IC₂₀ instead of hERG IC₅₀ for this very reason, and it is worth noting that in our assays 1 achieves 18% inhibition at 30 μM in the automated QPatch assay. For the clinical compounds in Table 7, the iCSI ranges from greater than

**Figure 8.** Tumor volumes and body weight changes in the HCT-116 human colon xenograft model in athymic female nude mice following treatment with vehicle or 25i at 25 or 50 mg/kg. Treatments were initiated on day 12 post implantation when mean tumor volume reached approximately 193 mm³. 25i was administered in tartaric acid, iv, qd for 13 total doses. Data is expressed as mean \pm standard error of the mean (SEM). $p < 0.05$ compared to vehicle controls using a one-way ANOVA.**Table 6.** Comparison of the in Vivo Efficacy of 11r and 25i with 1 and 3 in the HCT116 Xenograft Model

compd	dose ^a (mg/kg)	duration (days)	% T/C	% regressions	body wt change (% yield)	survive total
vehicle			100		−1.8	8/8
1	150 ip ^b	21	43		NR	NR
3	100	14	20		1.4	8/8
11r	10	8		22	>15	8/8
	10	8		52	>15	8/8
25i	25	13	10		−14.2	8/8
	50	13		9	−14.8	8/8

^a Dosed iv on a QD schedule. ^b Dosed ip on a QD schedule (data from NDA no. 21991 study report PD005, FDA submission). NR: not reported.

Table 7. Comparison of Cellular Activity and iCSI of 11r, 25f, and 25i with Select Clinical HDAC Inhibitors

compd	IC ₅₀ (nM)			hERG inhibition at 30 μM (%)	iCSI ^d
	HCT116	H1299	hERG ^a		
1	810	8200	>30,000	18	>37
2	160	460	>30,000	18	>188
3	15	100	10,300 ^b	57	542
5	310	1440	>30,000	30	>97
6	670	>4000	>30,000	38	>45
11r	4	26	>30,000 ^b	5 ^c	>7500
25f	3.4	21	>30,000	34	>9000
25i	4.5	29	>30,000	31	>7000

^a Automated Q-patch assay. ^b Manual patch clamp. ^c Manual patch clamp % inhibition at 10 μM . ^d iCSI calculated from HCT116 cellular data.

37-fold for 1 to greater than 542-fold for 3. Compounds 11r, 25f, and 25i have at least another order of magnitude improvement in their CSI relative to 3. Combined with the enhanced potency of the compounds in this series, the iCSI of at least 4 orders of magnitude suggests that with a suitable ADME profile, these compounds might be able to effectively inhibit HDAC-1 without

significant hERG blockade in vivo. By employing iCSI as a decision making tool during lead optimization, compounds were selected for in vivo studies that ultimately allowed toxicology studies to understand which cardiac observations may be off-target and which may be directly attributable to HDAC inhibition in vivo.

CONCLUSIONS

In conclusion, utilizing previously published approaches to mitigate hERG affinity in a series of hydroxamate based HDAC inhibitors, it was discovered that the pharmacophore for these two targets share a high degree of similarity and were not readily differentiated. A new approach toward reducing hERG activity was required and a more targeted approach utilizing homology models was employed. Compounds **11r** and **25i** were discovered through a novel approach of seeking divergence between the hERG and HDAC homology models based on the targeted introduction of amphiphilicity. This tactic may have broader application to other scaffolds that are recalcitrant to hERG optimizations, but the reliability of this approach needs to be evaluated more extensively before any general conclusions can be made. Analogues with an improved iCSI were generated and found to be efficacious in mouse tumor xenograft models. When compared to several HDAC inhibitors in clinical trials, **11r** and **25i** are more potent, efficacious, and provide a greater in vitro cardiac safety margin with which the QT effects observed in clinical trials could be investigated in preclinical safety models with the aim of translating these findings into a clinical setting. Further work in this area is ongoing, and the results of these studies will be published in due course.

EXPERIMENTAL SECTION

Materials and Methods. *Manual Patch Clamp Electrophysiology.* Cell culture: HEK293 cells stably transfected with the α -subunits of the hERG (University of Wisconsin, USA) were continuously maintained and passaged using standard cell culture media (Gibco-BRL, Switzerland) For experiments, the cells were plated onto sterile glass coverslips in 35 mm² dishes at a density of $1.1\text{--}1.5 \times 10^5$ cells per dish. The dishes were stored in a humidified and gassed (5% CO₂) incubator at 37 °C until use.

Test system: The effect on hERG currents was assessed by means of the patch clamp technique in the whole-cell configuration at 35 ± 2 °C. The corresponding vehicle for all superfusion concentrations was 0.1% DMSO. The vehicle effect was investigated in 5 cells. The effect of the positive controls 100 nM E-4031 (Calbiochem, Switzerland) was investigated in 2 cells. Cells were exposed to the test item for approximately 10 min of hERG tail currents were elicited by voltage jumps from -75 mV to $+10$ mV (500 ms) and then to -40 mV (500 ms) at 0.1 Hz. The composition of the extracellular solutions was [mM]: NaCl 137; KCl 4; CaCl₂ 1.8; MgCl₂ 1.0; D-glucose 10; N-2-hydroxyethylpiperazine-*N'*-2-ethanesulfonic acid (HEPES) 10; pH 7.4 (adjusted with 5 M NaOH). The composition of the pipet solutions was (mM): KCl 130; MgCl₂ 1.0; ethylene glycol-bis(ss-aminoethyl ether)-*N,N,N',N'*-tetraacetic acid (EGTA) 5; Mg-ATP 5; HEPES 10; pH 7.2 (adjusted with 1 M KOH). The compound effect on the currents was corrected by the mean vehicle rundown which was observed ($n = 5$) in the two cell lines. Data capturing and analysis was performed by using Pulse (Heka Electronics, Germany) and Excel.

Enzymatic, cellular, and in vivo efficacy studies were performed as previously described.⁵²

Compounds **6**, **11a**, **11b**, **11f**, **11k**, **11l**, **11n**, **11p**, and **11q** were prepared as previously described. The purity of all compounds was determined using high resolution HPLC/MS characterization and found to be >95% pure except as noted. High resolution LC/ESI-MS data were recorded using an Agilent 6220 mass spectrometer with electrospray ionization source and an Agilent 1200 liquid chromatograph with a gradient from 5% to 95% acetonitrile in water on a C18 reverse phase column with a diode array detection. The resolution of the MS system was approximately 11000 (fwhm definition). HPLC separation was performed using one of the methods (denoted in the header text) listed at end of report. Purine and hexakis(1*H*,1*H*,3*H*-tetrafluoropropoxy)phosphazine (protonated molecules *m/z* 121.05087 and 922.00979, respectively) were used as a reference. The mass accuracy of the system has been found to be <2 ppm.

Method A. Typical procedure for reductive amination using NaBH(OAc)₃:

To a solution of the tryptamine analogue (1 mmol) and (*E*)-3-(4-formyl-phenyl)-acrylic acid methyl ester (0.96 mmol) in THF (4 mL) was added solid NaHCO₃ (2.5 mmol), and the mixture was stirred for 48 h at ambient temperature. NaBH(OAc)₃ (1.4 mmol) was then added and the mixture was stirred until judged complete by LCMS analysis, typically 5–16 h. It was quenched with aqueous NH₄Cl and washed with excess EtOAc (2×). The combined organic layers were dried (MgSO₄), filtered, concentrated, and purified by silica gel chromatography.

Method B. Typical procedure for the conversion of esters to hydroxamic acids:

To a stirred solution of a methyl ester (4 mmol) in methanol (5 mL) at 0 °C was added sodium methoxide (5 equiv, 20 mmol of a 25% solution in methanol) and 10 equiv of hydroxylamine (50% solution in water). The reaction is monitored by LCMS, and upon completion the reaction mixture was brought to pH 7–8 with 1 N hydrochloric acid whereupon a precipitate formed. The solid is filtered, washed with water, and dried in vacuo to yield the desired hydroxamic acid.

Method C. Typical procedure for the formation of 3-dimethylaminomethyl azaindoles:

A mixture of azaindole (22 mmol), dimethylamine hydrochloride (2.0 g, 25 mmol), and paraformaldehyde (0.75 g, 2.5 mmol) in 1-butanol (60 mL) were stirred at reflux for 3 h. The resulting solution was evaporated in vacuo and purified via flash column chromatography.

Method D. Typical procedure for the formation of 3-azaindole acetonitriles from 3-dimethylaminomethyl indoles:

Sulfuric acid dimethyl ester (2.1 g, 16 mmol) was added to a solution of dimethyl 3-azindolmethyl-amine (15 mmol) in THF (12 mL). The mixture was stirred at reflux for 30 min. The solution was then placed in an ice bath, and most of the THF is decanted out to give a gummy intermediate which was washed several times with ether. Water (6 mL) and sodium cyanide (950 mg, 19 mmol) were added, and the solution was then stirred at reflux for 1 h. Upon completion of the reaction, the solution was cooled and extracted with EtOH:DCM (1:4) several times. The combined organic layers were washed with brine and dried over Na₂SO₄. The organic solvent was removed to provide crude product, which was purified via flash column chromatography (MeOH:DCM, 1:99 to 20:90).

Method E. (2-Methyl-1*H*-indol-3-yl)-acetaldehyde. Starting with (2-methyl-1*H*-indol-3-yl)-acetic acid ethyl ester (4.0 g, 18 mmol) the title compound (2.3 g, 74% yield) was prepared according to the previously described procedure.⁶⁹ ¹H NMR (400 MHz, CDCl₃) δ 9.69 (t, *J* = 2.9 Hz, 1 H), 7.99 (br, 1 H), 7.48 (d, *J* = 7.5 Hz, 1 H), 7.33 (d, *J* = 8.0 Hz, 1 H), 7.16 (ddt, *J* = 19.6, 10.4, 3.7 Hz, 2 H), 3.74 (d, *J* = 3.0 Hz, 2 H), 2.42 (s, 3 H). MS *m/z* 174.1 (MH⁺).

(*E*)-3-{4-[(2-Fluoro-ethylamino)-methyl]-phenyl}-acrylic Acid Methyl Ester (**8c**). 2-Fluoro-ethylamine hydrochloride (110 mg, 1.1 mmol) was added to a solution of (*E*)-3-(4-formyl-phenyl)-acrylic acid methyl ester (**7**) (200 mg, 1.1 mmol) and acetic acid (0.5 mL) in DMF (2 mL) at

room temperature. The mixture was stirred at room temperature for 10 min. SiliaBond cyanoborohydride (1.1 g, 1.1 mmol, 1 g/mmol) was added and stirred at room temperature for another 10 min. The mixture was then heated via microwave irradiation at 150 °C for 5 min, filtered, and concentrated under vacuum. The crude product was purified via flash column chromatography (EtOAc:hexanes, 10:90 to 100:0; MeOH:DCM, 1:99 to 10:90) to provide product (100 mg, 38% yield). ¹H NMR (400 MHz, CDCl₃) δ 7.70 (d, *J* = 15.9 Hz, 1 H), 7.50 (d, *J* = 8.1 Hz, 2 H), 7.42 (d, *J* = 8.2 Hz, 2 H), 6.44 (d, *J* = 16.0 Hz, 1 H), 4.55 (dt, *J* = 47.7, 5.0 Hz, 2 H), 3.83 (s, 3 H), 3.72 (s, 2 H), 2.82 (dt, *J* = 26.9, 5.1 Hz, 2 H). MS *m/z* 238.2 (MH⁺).

(*E*)-3-[4-[(2,2-Difluoro-ethylamino)-methyl]-phenyl]-acrylic Acid Methyl Ester (**8d**). Starting from 2,2-difluoro-ethylamine (250 mg, 3.1 mmol) the title compound was prepared following the procedure for **8c** (550 mg, 70% yield). ¹H NMR (400 MHz, CD₃OD) δ 7.69 (d, *J* = 16.3 Hz, 1 H), 7.58 (d, *J* = 8.3 Hz, 2 H), 7.40 (d, *J* = 8.3 Hz, 2 H), 6.52 (d, *J* = 15.6 Hz, 1 H), 5.90 (tt, *J* = 56.3, 4.3 Hz, 1 H), 3.84 (s, 2 H), 3.78 (s, 3 H), 2.90 (td, *J* = 15.6, 4.6 Hz, 2 H). MS *m/z* 256.1 (MH⁺).

(*E*)-3-[4-[(3,3-Difluoro-propylamino)-methyl]-phenyl]-acrylic Acid Methyl Ester (**8g**). Starting from 3,3-difluoro-propylamine hydrochloride (250 mg, 2.1 mmol) the title compound was prepared following the procedure for **8c** (460 mg, 81% yield). MS *m/z* 270.1 (MH⁺).

(*E*)-3-[4-[(2-Fluoro-ethyl)-[2-(2-methyl-1H-indol-3-yl)-ethyl]-amino]-methyl]-phenyl]-acrylic Acid Methyl Ester (**9c**). Following method A, the title compound (100 mg, 60% yield) was prepared from **8c** (100 mg, 0.42 mmol) and (2-methyl-1H-indol-3-yl)-acetaldehyde (80 mg, 0.46 mmol). ¹H NMR (400 MHz, CDCl₃) δ 7.80 (s, 1 H), 7.74 (d, *J* = 15.9 Hz, 1 H), 7.49 (d, *J* = 8.9 Hz, 2 H), 7.40 (d, *J* = 8.0 Hz, 2 H), 7.38 (d, *J* = 7.3 Hz, 1 H), 7.26 (d, *J* = 8.1 Hz, 1 H), 7.13 (t, *J* = 7.5 Hz, 1 H), 7.06 (t, *J* = 7.5 Hz, 1 H), 6.48 (d, *J* = 15.7 Hz, 1 H), 4.58 (dt, *J* = 47.6, 5.3 Hz, 2 H), 3.86 (s, 3 H), 3.83 (s, 2 H), 3.01–2.78 (m, 6 H), 2.32 (s, 3 H). MS *m/z* 395.2 (MH⁺).

(*E*)-3-[4-[(2,2-Difluoro-ethyl)-[2-(2-methyl-1H-indol-3-yl)-ethyl]-amino]-methyl]-phenyl]-acrylic Acid Methyl Ester (**9d**). Following method A, the title compound (400 mg, 81% yield) was prepared from **8d** (550 mg, 2.1 mmol) and (2-methyl-1H-indol-3-yl)-acetaldehyde (200 mg, 1.2 mmol). ¹H NMR (400 MHz, CDCl₃) δ 7.75 (br, 1 H), 7.72 (d, *J* = 15.8 Hz, 1 H), 7.49 (d, *J* = 7.9 Hz, 2 H), 7.41–7.37 (m, 2 H), 7.34 (d, *J* = 7.8 Hz, 1 H), 7.27 (d, *J* = 8.2 Hz, 1 H), 7.11 (td, *J* = 7.5, 1.3 Hz, 1 H), 7.04 (td, *J* = 7.5, 0.9 Hz, 1 H), 6.46 (d, *J* = 15.6 Hz, 1 H), 5.81 (t, *J* = 56.2 Hz, 1 H), 3.85 (s, 2 H), 3.84 (s, 3 H), 3.00 (td, *J* = 14.4, 3.8 Hz, 2 H), 2.89–2.83 (m, 4 H), 2.32 (s, 3 H). MS *m/z* 413.2 (MH⁺).

(*E*)-3-[4-[(2-(1H-Indol-3-yl)-ethyl)-[2,2,2-trifluoro-ethyl]-amino]-methyl]-phenyl]-acrylic Acid Methyl Ester (**9e**). 2,2,2-Trifluoro-ethane-1,1-diol (100 mg, 0.90 mmol) and *p*-toluenesulfonic acid (6 mg, 0.03 mmol) were added to a solution of (*E*)-3-[4-[(2-(1H-indol-3-yl)-ethylamino)-methyl]-phenyl]-acrylic acid methyl ester (200 mg, 0.60 mmol) in toluene (2 mL). The mixture was stirred at reflux temperature under Dean–Stark trap. Upon the completion of reaction, THF (2 mL) and sodium triacetoxyborohydride (150 mg, 0.72 mmol) were added. The resulting mixture was stirred at room temperature, and then sodium bicarbonate solution was added. The aqueous layer was extracted several times with EtOAc. The combined organic layer was washed with brine, dried over Na₂SO₄, filtered, and concentrated. The resulting crude product was purified via flash column chromatography to afford a white powder (215 mg, 86% yield). ¹H NMR (CDCl₃) δ ppm 8.0 (br s, 1H), 7.72 (d, *J* = 16.0 Hz, 1 H), 7.61 (d, *J* = 8.6 Hz, 1 H), 7.54 (m, 4 H), 7.41 (d, *J* = 8.2 Hz, 1 H), 7.29 (m, 2 H), 7.20 (d, *J* = 7.7 Hz, 1 H), 6.48 (d, *J* = 16.0 Hz, 1 H), 4.29 (br s, 1 H), 4.14 (m, 5 H), 3.91 (s, 1 H), 3.84 (s, 4 H), 3.56 (m, 1 H), 3.35 (m, 1 H), 3.07 (br s, 1 H), 2.78 (m, 1 H), 2.07 (m, 2 H), 1.8 (m, 1 H).

(*E*)-3-[4-[(3,3-Difluoro-propyl)-[2-(2-methyl-1H-indol-3-yl)-ethyl]-amino]-methyl]-phenyl]-acrylic Acid Methyl Ester (**9g**). Following method A, the title compound (380 mg, 74% yield) was prepared from

8g (460 mg, 1.7 mmol) and (2-methyl-1H-indol-3-yl)-acetaldehyde (200 mg, 1.2 mmol). ¹H NMR (400 MHz, CDCl₃) δ 7.90 (br, 1 H), 7.74 (d, *J* = 16.0 Hz, 1 H), 7.51 (d, *J* = 8.4 Hz, 2 H), 7.40 (d, *J* = 8.0 Hz, 2 H), 7.32 (d, *J* = 7.8 Hz, 1 H), 7.24 (dt, *J* = 8.0, 0.9 Hz, 1 H), 7.10 (ddd, *J* = 8.1, 7.0, 1.2 Hz, 1 H), 7.03 (ddd, *J* = 7.8, 7.0, 1.0 Hz, 1 H), 6.48 (d, *J* = 15.9 Hz, 1 H), 3.87 (s, 2 H), 3.85 (s, 3 H), 2.96 (t, *J* = 13.2 Hz, 2 H), 2.89–2.79 (m, 4 H), 2.29 (s, 3 H), 1.65 (t, *J* = 18.8 Hz, 3 H). MS *m/z* 427.2 (MH⁺).

(*E*)-3-[4-[(2-(1H-Indol-3-yl)-ethyl)-[3,3,3-trifluoro-propyl]-amino]-methyl]-phenyl]-acrylic Acid Methyl Ester (**9h**). Following method A, the title compound (160 mg, 41% yield) was prepared from **8h** (300 mg, 0.90 mmol) and 3,3,3-trifluoro-propionaldehyde (105 mg, 0.94 mmol). ¹H NMR (400 MHz, CDCl₃) δ 7.97 (s, 1 H), 7.71 (d, *J* = 16.1 Hz, 1 H), 7.49–7.46 (m, 3 H), 7.39–7.35 (m, 2 H), 7.20 (ddd, *J* = 8.1, 6.9, 1.3 Hz, 1 H), 7.09 (ddd, *J* = 8.0, 7.2, 1.0 Hz, 1 H), 7.00 (d, *J* = 2.9 Hz, 1 H), 6.46 (d, *J* = 16.3 Hz, 1 H), 3.84 (s, 3 H), 3.73 (s, 2 H), 2.99–2.93 (m, 2 H), 2.90–2.81 (m, 4 H), 2.36 (m, 2 H). MS *m/z* 431.2 (MH⁺).

(*E*)-3-[4-[(2-Fluoro-ethyl)-[2-(2-methyl-1H-indol-3-yl)-ethyl]-amino]-methyl]-phenyl]-N-hydroxy-acrylamide (**11c**). Following method B, the title compound (8.9 mg, 9.3% yield) was prepared from **9c** (100 mg, 0.24 mmol). ¹H NMR (400 MHz, CD₃OD) δ 7.56 (d, *J* = 15.6 Hz, 1 H), 7.54 (d, *J* = 7.6 Hz, 1 H), 7.41 (d, *J* = 7.9 Hz, 2 H), 7.29 (d, *J* = 8.1 Hz, 2 H), 7.25 (d, *J* = 8.3 Hz, 1 H), 7.02 (ddd, *J* = 8.1, 7.0, 1.1 Hz, 1 H), 6.93 (ddd, *J* = 8.1, 7.0, 1.1 Hz, 1 H), 6.56 (d, *J* = 16.0 Hz, 1 H), 4.63 (dt, *J* = 47.4, 5.4 Hz, 2 H), 3.86 (s, 2 H), 3.03 (dt, *J* = 26.8, 5.2 Hz, 2 H), 2.95–2.78 (m, 4 H), 2.32 (s, 3 H). MS *m/z* 396.2 (MH⁺). HRMS calcd for C₂₃H₂₆N₃O₂F (MH⁺) 396.2087, found 396.2092.

(*E*)-3-[4-[(2,2-Difluoro-ethyl)-[2-(2-methyl-1H-indol-3-yl)-ethyl]-amino]-methyl]-phenyl]-N-hydroxy-acrylamide (**11d**). Following method B, the title compound (180 mg, 46% yield) was prepared from **9d** (400 mg, 0.92 mmol). ¹H NMR (400 MHz, CD₃OD) δ 7.58 (d, *J* = 15.5 Hz, 1 H), 7.43 (d, *J* = 7.8 Hz, 2 H), 7.27 (d, *J* = 7.8 Hz, 2 H), 7.22 (d, *J* = 5.3 Hz, 1 H), 7.20 (d, *J* = 4.7 Hz, 1 H), 6.97 (t, *J* = 7.3 Hz, 1 H), 6.88 (t, *J* = 7.5 Hz, 1 H), 6.48 (d, *J* = 15.8 Hz, 1 H), 5.78 (tt, *J* = 56.2, 4.4 Hz, 1 H), 3.67 (s, 2 H), 2.88 (td, *J* = 14.9, 4.2 Hz, 2 H), 2.79–2.64 (m, 4 H), 2.23 (s, 3 H). MS *m/z* 414.2 (M + 1). ¹³C NMR (400 MHz, CD₃OD) δ 166.50, 142.87, 141.54, 137.11, 135.14, 132.62, 130.52, 129.89, 128.79, 121.22, 119.3, 118.35, 117.98, 111.24, 109.32, 60.26, 57.37 (t), 56.29, 49.46, 23.23, 11.35. HRMS calcd for C₂₃H₂₅N₃O₃F₂ (M⁺) 412.1837, found 412.1854.

(*E*)-N-Hydroxy-3-[4-[(2-(1H-indol-3-yl)-ethyl)-[2,2,2-trifluoro-ethyl]-amino]-methyl]-phenyl]-acrylamide (**11e**). Following method B, the title compound (26 mg, 19% yield) was prepared from **9e** (140 mg, 0.39 mmol). ¹H NMR (400 MHz, CD₃OD) δ 7.58 (d, *J* = 15.8 Hz, 1 H), 7.54 (d, *J* = 8.2 Hz, 2 H), 7.50 (d, *J* = 8.2 Hz, 1 H), 7.45 (d, *J* = 7.6 Hz, 2 H), 7.34 (d, *J* = 8.2 Hz, 1 H), 7.13 (t, *J* = 8.2 Hz, 1 H), 7.03 (t, *J* = 7.6 Hz, 1 H), 6.47 (d, *J* = 15.8 Hz, 1 H), 4.28 (q, *J* = 7.6 Hz, 1 H), 4.00 (d, *J* = 13.9 Hz, 1 H), 3.86 (d, *J* = 13.9 Hz, 1 H), 3.43 (m, 1 H), 3.15 (d, *J* = 13.2, 5.0 Hz, 1 H), 3.01 (m, 1 H), 2.61 (dd, *J* = 17.0, 3.2 Hz, 1 H). MS *m/z* (M + 1). ¹³C NMR (400 MHz, CD₃OD) δ 142.09, 141.40, 138.40, 135.56, 130.56, 128.88, 127.78, 125.07, 123.23, 119.98, 119.19, 118.25, 112.20, 111.90, 79.04, 59.01, 46.65, 17.72. HRMS calcd for C₂₂H₂₂N₃O₂F₃ (MH⁺) 418.1742, found 416.1611.

(*E*)-3-[4-[(3,3-Difluoro-propyl)-[2-(2-methyl-1H-indol-3-yl)-ethyl]-amino]-methyl]-phenyl]-N-hydroxy-acrylamide (**11g**). Following method B, the title compound (200 mg, 53% yield) was prepared from **9g** (380 mg, 0.85 mmol). ¹H NMR (400 MHz, CD₃OD) δ 7.59 (d, *J* = 15.4 Hz, 1 H), 7.51 (d, *J* = 7.9 Hz, 2 H), 7.38 (d, *J* = 8.2 Hz, 2 H), 7.21 (d, *J* = 3.4 Hz, 1 H), 7.19 (d, *J* = 3.7 Hz, 1 H), 6.96 (td, *J* = 7.5, 1.2 Hz, 1 H), 6.86 (td, *J* = 7.5, 1.3 Hz, 1 H), 6.48 (d, *J* = 15.3 Hz, 1 H), 3.81 (s, 2 H), 2.93 (t, *J* = 13.2 Hz, 2 H), 2.86–2.82 (m, 2 H), 2.75–2.71 (m, 2 H), 2.26 (s, 3 H), 1.58 (t, *J* = 19.2 Hz, 3 H). MS *m/z* 428.3 (MH⁺). HRMS calcd for C₂₄H₂₇N₃O₂F₂ (MH⁺) 428.2150, found 428.2148.

(*E*)-N-Hydroxy-3-[4-[(2-(1H-indol-3-yl)-ethyl)-[3,3,3-trifluoro-propyl]-amino]-methyl]-phenyl]-acrylamide (**11h**). Following method B, the title compound (33 mg, 21% yield) was prepared from **9h** (160 mg,

0.37 mmol). ^1H NMR (400 MHz, CD_3OD) δ 7.53–7.46 (m, 3 H), 7.37–7.31 (m, 4 H), 7.06 (ddd, J = 8.1, 7.1, 1.0 Hz, 1 H), 7.01 (s, 1 H), 6.94 (ddd, J = 8.0, 7.0, 1.1 Hz, 1 H), 6.49 (d, J = 15.7 Hz, 1 H), 3.68 (s, 2 H), 2.94–2.90 (m, 2 H), 2.85–2.76 (m, 4 H), 2.39–2.30 (m, 2 H). ^{13}C NMR (400 MHz, CD_3OD) δ 166.5, 142.7, 141.52, 138.15, 135.12, 130.6, 128.79, 127.08, 123.22, 122.2, 119.44, 119.23, 118.0, 114.02, 112.2, 59.11, 55.59, 49.38 (q), 47.60 (q), 32.45 (q), 24.20. MS m/z 432.2 (MH^+). HRMS calcd for $\text{C}_{23}\text{H}_{24}\text{N}_3\text{O}_2\text{F}_3$ (MH^+) 432.1899, found 432.1901.

3-(2-Amino-ethyl)-1H-indole-2-carboxylic Acid Ethyl Ester Hydrochloride (14). Starting from 2-(3-chloro-propyl)-malonic acid diethyl ester (11.8 g, 49.9 mmol) the title compound (4.4 g, 33% yield) was prepared according to the procedure as previously described.⁷⁰ ^1H NMR (400 MHz, $\text{DMSO}-d_6$) δ 8.15 (br, 2 H), 7.79 (d, J = 8.3 Hz, 1 H), 7.45 (d, J = 8.7 Hz, 1 H), 7.29 (t, J = 7.6 Hz, 1 H), 7.11 (t, J = 7.5 Hz, 1 H), 4.38 (q, J = 7.1 Hz, 2 H), 3.38 (m, 2 H), 1.42–1.34 (m, 5 H). MS m/z 233 (MH^+).

3-{2-[4-((E)-2-Methoxycarbonyl-vinyl)-benzylamino]-ethyl}-1H-indole-2-carboxylic Acid Ethyl Ester (9j). Following method A, the title compound was prepared from **14**. ^1H NMR (400 MHz, CDCl_3) δ 8.67 (s, 1 H), 7.64 (dd, J = 8.1, 1.1 Hz, 1 H), 7.57 (d, J = 16.2 Hz, 1 H), 7.37 (d, J = 8.0 Hz, 2 H), 7.29 (ddd, J = 9.2, 8.1, 1.2 Hz, 1 H), 7.24 (d, J = 8.0 Hz, 2 H), 7.07 (ddd, J = 8.1, 6.7, 1.2 Hz, 1 H), 6.31 (d, J = 16.0 Hz, 1 H), 4.32 (q, J = 7.2 Hz, 2 H), 3.79 (s, 2 H), 3.73 (s, 3 H), 3.28 (t, J = 7.4 Hz, 2 H), 2.91 (t, J = 7.6 Hz, 2 H), 1.32 (t, J = 7.5 Hz, 3 H). MS m/z 313.2 ($\text{M} + 1$).

3-{2-[4-((E)-2-Hydroxycarbonyl-vinyl)-benzylamino]-ethyl}-1H-indole-2-carboxylic Acid (11j). Powdered sodium hydroxide (100 mg, 2.5 mmol) was added to a solution of **9j** (190 mg, 0.47 mmol) and hydroxylamine (0.16 mL, 5 mmol, 50% in water) in ethanol (3 mL). The mixture was stirred at room temperature overnight and purified via preparative HPLC to give both the title compound (13 mg, 7% yield) and (E)-N-hydroxy-3-[4-(1-oxo-1,3,4,9-tetrahydro- β -carbolin-2-ylmethyl)-phenyl]-acrylamide (9.5 mg, 5% yield). ^1H NMR (400 MHz, CD_3OD) δ 7.59 (dt, J = 8.0, 1.0 Hz, 1 H), 7.54 (d, J = 15.9 Hz, 1 H), 7.49 (d, J = 7.9 Hz, 2 H), 7.41 (dt, J = 8.2, 1.0 Hz, 1 H), 7.32 (d, J = 8.4 Hz, 2 H), 7.23 (ddd, J = 8.3, 7.0, 1.3 Hz, 1 H), 7.08 (ddd, J = 8.0, 6.9, 1.2 Hz, 1 H), 6.46 (d, J = 15.8 Hz, 1 H), 3.80 (s, 2 H), 3.24 (t, J = 6.5 Hz, 2 H), 3.07 (t, J = 6.1 Hz, 2 H). MS m/z 380.1 ($\text{M} + 1$).

(2-Bromo-1H-indol-3-yl)-acetonitrile. To a solution of (1H-indol-3-yl)-acetonitrile (5.0 g, 32.0 mmol) in DCM (300 mL) under N_2 atmosphere was slowly added N-bromosuccinimide (5.98 g, 33.6 mmol), and the mixture was stirred for 30 min at ambient temperature. The reaction mixture was added with hexane, and the solvents were evaporated in vacuo (with no heat) and more hexane was added to make a slurry. The suspension was transferred to the top of a large SiO_2 plug and filtered with 0–30% EtOAc in hexanes to give the title compound (5.03 g, 21.4 mmol, 67% yield) as a brown oil. ^1H NMR (CDCl_3) δ 8.23 (br s, 1H), 7.63 (d, J = 8.1 Hz, 1H), 7.32 (m, 1H), 7.22 (m, 2H), 3.79 (s, 2H); m/z 236.8 (MH^+).

[2-(4-Methoxy-pyridin-3-yl)-1H-indol-3-yl]-acetonitrile (12m). In an oven-dried pressure tube under N_2 atmosphere were taken (2-bromo-1H-indol-3-yl)-acetonitrile (100 mg, 0.43 mmol), 2-methoxy-5-pyridine boronic acid (130 mg, 0.85 mmol), and K_2CO_3 (88 mg, 0.64 mmol) in toluene (4 mL), and N_2 was bubbled through the suspension for 10 min. Then tetrakis(triphenylphosphine)palladium (49 mg, 0.04 mmol) was added to it, and the tube was sealed. The mixture was heated to 90 °C for 16 h, filtered through a Celite plug, and the plug was washed further with more DCM. All the filtrates were combined together and concentrated to a crude oil that was purified by flash column (0–30% EtOAc in heptane) to give the title compound (59 mg, 0.22 mmol, 53% yield) as a light-yellow oil. ^1H NMR (CDCl_3) δ 8.37 (d, J = 2.3 Hz, 1H), 8.26 (br s, 1H), 7.77 (dd, J = 2.5, 8.5 Hz, 1H), 7.73 (d, J = 7.7 Hz, 1H), 7.45 (d, J = 7.9 Hz, 1H), 7.29 (m, 2H), 6.93 (d, J = 8.5 Hz, 1H), 4.04 (s, 3H), 3.87 (s, 2H). m/z 263.9 (MH^+).

[2-(3,5-Dimethyl-isoxazol-4-yl)-1H-indol-3-yl]-acetonitrile (12o). To a solution of (2-bromo-1H-indol-3-yl)-acetonitrile (2.0 g, 8.51 mmol) in toluene (15 mL) in a dry pressure tube under N_2 were added 3,5-dimethyl-isoxazol-4-boronic acid (1.32 g, 9.36 mmol), tris(dibenzylidenedipalladium) (0.78 g, 0.85 mmol), tri-*tert*-butylphosphonium tetrafluoroborate (0.49 g, 1.70 mmol), and potassium fluoride (1.48 g, 25.5 mmol), and the suspension was bubbled with N_2 . The tube was sealed and the mixture was heated to 50 °C for 16 h. The crude material was diluted with EtOAc and filtered through a Celite plug. The filtrate was concentrated and purified by column (0–40% EtOAc in heptane) to give the title compound (1.35 g, 5.37 mmol, 63% yield) as a yellow solid. ^1H NMR (CDCl_3) δ 8.21 (br s, 1H), 7.74 (d, J = 7.7 Hz, 1H), 7.44 (d, J = 8.0 Hz, 1H), 7.30 (m, 2H), 3.66 (s, 2H), 2.41 (s, 3H), 2.23 (s, 3H). m/z 251.9 (MH^+).

2-[2-(4-Methoxy-pyridin-3-yl)-1H-indol-3-yl]-ethylamine (13m). In a dry Parr bottle was dissolved **12m** (592 mg, 2.25 mmol) in EtOH (15 mL). Then aqueous NH_4OH (7.5 mL) followed by rhodium on alumina (400 mg) were added to the mixture and stirred at room temperature for 40 h under 45 psi of H_2 pressure when LCMS showed complete product formation. The reaction mixture was filtered through a Celite pad, and the pad was washed with excess MeOH. The combined filtrates were concentrated to give the title compound (590 mg, 2.21 mmol, 98% yield) as a crude yellow–brown solid that was used in the next step directly. ^1H NMR (CD_3OD) δ 8.40 (m, 1H), 7.94 (dd, J = 2.3, 8.5 Hz, 1H), 7.63 (d, J = 7.9 Hz, 1H), 7.42 (d, J = 7.9 Hz, 1H), 7.19 (m, 1H), 7.11 (m, 1H), 6.98 (d, J = 8.7 Hz, 1H), 4.01 (s, 3H), 3.23 (m, 4H). m/z 267.9 (MH^+).

2-[2-(3,5-Dimethyl-isoxazol-4-yl)-1H-indol-3-yl]-ethylamine (13o). To a solution of **12o** (830 mg, 3.3 mmol) in THF (20 mL) was added $\text{BH}_3 \cdot \text{THF}$ (9.9 mL, 1M, 9.9 mmol), and the mixture was stirred for 5 h at ambient temperature. It was then cooled in ice bath and quenched with MeOH. The crude material was concentrated to an oil, combined with 5 mL of aqueous 6N NaOH solution and stirred for 30 min. Then EtOAc was added and the layers were separated. The aqueous layer was washed twice with EtOAc, and the combined organic layers were dried with MgSO_4 , concentrated, and purified by flash column (100% EtOAc, then 10% MeOH in DCM with a few drops of NH_4OH) to give the title compound (388 mg, 1.52 mmol, 48% yield, 90% pure) as a crude brown solid. ^1H NMR (CD_2Cl_2) δ 8.31 (br s, 1H), 7.67 (d, J = 8.6 Hz, 1H), 7.41 (d, J = 7.9 Hz, 1H), 7.24 (m, 1H), 7.15 (m, 1H), 3.44 (s, 1H), 2.89 (m, 2H), 2.77 (m, 2H), 2.36 (s, 3H), 2.20 (s, 3H). m/z 255.9 (MH^+).

(E)-3-[4-({2-[2-(4-Methoxy-pyridin-3-yl)-1H-indol-3-yl]-ethylamino}-methyl)-phenyl]-acrylic Acid Methyl Ester (8m). Following method A, **20m** (200 mg, 0.75 mmol) was converted to the title compound (120 mg, 0.27 mmol, 36% yield) as a yellow oil. ^1H NMR (CDCl_3) δ 8.41 (m, 1H), 8.08 (br s, 1H), 7.83 (m, 1H), 7.63 (m, 2H), 7.40 (m, 3H), 7.30 (m, 2H), 7.24 (m, 1H), 7.16 (m, 1H), 6.86 (d, J = 8.5 Hz, 1H), 6.37 (d, J = 15.8 Hz, 1H), 4.02 (s, 3H), 3.83 (m, 5H), 3.05 (m, 4H). m/z 441.9 (MH^+).

(E)-3-[4-({2-[2-(3,5-Dimethyl-isoxazol-4-yl)-1H-indol-3-yl]-ethylamino}-methyl)-phenyl]-acrylic Acid Methyl Ester (8o). Following method A, **20o** (279 mg, 1.09 mmol) was converted to the title compound (142 mg, 0.33 mmol, 36% yield) as a yellow oil. ^1H NMR (CDCl_3) δ 7.65 (m, 2H), 7.42 (d, J = 7.7 Hz, 2H), 7.37 (d, J = 7.7 Hz, 1H), 7.23 (m, 3H), 7.14 (m, 1H), 6.40 (d, J = 16.5 Hz, 1H), 3.79 (s, 3H), 3.73 (s, 2H), 2.84 (br s, 2H), 2.25 (s, 3H), 2.10 (s, 3H). m/z 430.1 (MH^+).

(E)-N-Hydroxy-3-[4-({2-[2-(4-methoxy-pyridin-3-yl)-1H-indol-3-yl]-ethylamino}-methyl)-phenyl]-acrylamide (11m). Following method B, **8m** (120 mg, 0.27 mmol) was converted to the title compound (46 mg, 0.10 mmol, 38% yield) as a yellow solid after HPLC purification. ^1H NMR (CD_3OD) δ 8.35 (s, 1H), 7.86 (d, J = 8.9 Hz, 1H), 7.54 (d, J = 7.6 Hz, 1H), 7.46 (m, 3H), 7.37 (d, J = 8.0 Hz, 1H), 7.23 (d, J = 7.8 Hz, 1H), 7.13 (m, 1H), 7.02 (m, 1H), 6.88 (d, J = 8.9 Hz, 1H), 6.48 (d, J = 15.6 Hz, 1H), 3.97 (s, 3H), 3.73 (s, 2H), 3.09 (m, 2H), 2.85 (m, 2H).

^{13}C NMR (CD_3OD) δ 166.13, 164.86, 146.95, 141.95, 140.06, 139.11, 137.96, 135.68, 132.97, 130.17, 129.94, 128.65, 124.37, 122.97, 120.15, 119.63, 119.53, 112.08, 111.72, 110.75, 54.27, 53.69, 50.18, 25.41. m/z 443.1 (MH^+). HRMS (MH^+) calcd for $\text{C}_{26}\text{H}_{26}\text{N}_4\text{O}_3$, 443.2083, found 443.2074.

(*E*)-3-[4-[(2-[2-(3,5-Dimethyl-isoxazol-4-yl)-1*H*-indol-3-yl]-ethylamino)-methyl]-phenyl]-*N*-hydroxy-acrylamide (**11o**). Following method B, **8o** (180 mg, 0.42 mmol) was converted to the title compound (145 mg, 0.337 mmol, 80% yield) TFA salt as a yellow solid after RP-HPLC purification. ^1H NMR (CD_3OD) δ 7.61 (m, 4H), 7.46 (d, J = 8.1 Hz, 2H), 7.38 (d, J = 7.7 Hz, 1H), 7.19 (m, 1H), 7.10 (m, 1H), 6.53 (d, J = 15.3 Hz, 1H), 4.23 (s, 2H), 3.18 (m, 2H), 3.04 (m, 2H), 2.34 (s, 3H), 2.17 (s, 3H). ^{13}C NMR (CD_3OD) δ 169.4, 165.9, 161.2, 140.4, 138.4, 137.5, 134.1, 131.5, 131.4, 129.7, 129.5, 128.6, 125.3, 123.6, 120.6, 120.0, 119.2, 112.5, 110.3, 109.9, 51.7, 23.0, 11.6, 10.5. m/z 430.9 (MH^+). HRMS (MH^+) calcd for $\text{C}_{25}\text{H}_{26}\text{N}_4\text{O}_3$, 431.2083, found 431.2085.

2-(3-{2-[(4-Bromo-benzyl)-isopropyl-amino]-ethyl}-1*H*-indol-2-yl)-propan-2-ol (**15**). 3-[2-(4-Bromo-benzylamino)-ethyl]-1*H*-indole-2-carboxylic acid ethyl ester: 3-(2-Amino-ethyl)-1*H*-indole-2-carboxylic acid ethyl ester hydrochloride (8.5 g, 27 mmol) was added to a solution of 4-bromo-benzaldehyde (4.7 g, 26 mmol) and acetic acid (2.3 mL, 41 mmol) in THF (120 mL). The mixture was stirred at room temperature for 1 h. To this mixture, sodium triacetoxyborohydride (8.4 g, 38 mol) was added, and the reaction mixture was stirred at room temperature overnight. Satd NaHCO_3 solution was added, and the aqueous layer was extracted with EtOAc several times. The organic layer was combined, dried over Na_2SO_4 , filtered, and evaporated off. The crude product was purified via flash column chromatography (EtOAc:hexanes, 10:90 to 60:40) to provide product (9 g, 83% yield). ^1H NMR (400 MHz, CDCl_3) δ 8.77 (br, 1 H), 7.72 (d, J = 8.2 Hz, 1 H), 7.54–7.09 (m, 7 H), 4.39 (q, J = 7.0 Hz, 2 H), 3.88 (s, 2 H), 3.42 (t, J = 7.2 Hz, 2 H), 3.06 (t, J = 7.0 Hz, 2 H), 1.40 (t, J = 7.2 Hz, 3 H). MS m/z 402 (MH^+).

3-[2-[(4-Bromo-benzyl)-isopropyl-amino]-ethyl]-1*H*-indole-2-carboxylic acid ethyl ester: 3-[2-(4-Bromo-benzylamino)-ethyl]-1*H*-indole-2-carboxylic acid ethyl ester (9.0 g, 222 mmol) was added to a solution of 2-iodo-propane (76 g, 448 mmol) and triethylamine (62 mL, 448 mmol) in CH_3CN (200 mL). The mixture was refluxed overnight. The solvent was then removed under vacuum. EtOAc and water were added. The aqueous layer was extracted several times with EtOAc. The combined organic layer was washed with brine, dried over Na_2SO_4 , filtered, and concentrated in vacuo. The crude product was purified via flash column chromatography (EtOAc:hexanes, 10:90 to 90:10) to provide slightly yellow solid (6.5 g, 65% yield). ^1H NMR (400 MHz, CDCl_3) δ 8.64 (br, 1 H), 7.45 (d, J = 8.3 Hz, 1 H), 6.87–7.27 (m, 4 H), 7.15 (d, J = 8.1 Hz, 2 H), 7.09 (t, J = 7.5 Hz, 1 H), 4.35 (q, J = 7.1 Hz, 2 H), 3.59 (s, 2 H), 3.18 (t, J = 7.9 Hz, 2 H), 2.09–2.00 (m, 1 H), 2.69 (t, J = 7.5 Hz, 2 H), 1.37 (t, J = 7.3 Hz, 3 H), 1.02 (d, J = 6.9 Hz, 6 H). MS m/z 444 (MH^+).

Methyl lithium (18 mL, 44 mmol, 2.5 M in diethoxymethane) was added to a solution of 3-[2-[(4-bromo-benzyl)-isopropyl-amino]-ethyl]-1*H*-indole-2-carboxylic acid ethyl ester (6.5 g, 15 mmol) in THF (65 mL) at -65°C . The mixture was stirred at same temperature for 2 h. Ice water was added slowly. The aqueous layer was then extracted several times with EtOAc. The combined organic layer was washed with brine, dried over Na_2SO_4 , filtered, and evaporated off. The crude product was purified via flash column chromatography (EtOAc:hexanes, 10:90 to 100:0) to provide yellow oil (5.5 g, 87% yield). ^1H NMR (400 MHz, CDCl_3) δ 8.05 (s, 1 H), 7.32 (d, J = 7.9 Hz, 1 H), 6.78–6.73 (m, 3 H), 6.64–6.60 (m, 3 H), 6.54 (t, J = 7.3 Hz, 1 H), 3.44 (s, 2 H), 3.01–2.94 (m, 1 H), 2.89 (t, J = 7.0 Hz, 2 H), 2.68 (t, J = 6.9 Hz, 2 H), 1.58 (s, 6 H), 1.01 (d, J = 6.7 Hz, 6 H). MS m/z 430 (MH^+).

(*E*)-3-[4-[(2-[2-(1-Hydroxy-1-methyl-ethyl)-1*H*-indol-3-yl]-ethyl)-isopropyl-amino)-methyl]-phenyl]-acrylic Acid Methyl Ester (**16**).

2-(3-{2-[(4-Bromo-benzyl)-isopropyl-amino]-ethyl}-1*H*-indol-2-yl)-propan-2-ol (5.0 g, 12 mmol) was added to a suspension of tris-(dibenzylideneacetone)dipalladium(0) (100 mg, 0.12 mmol) and tributylphosphine tetrafluoroborate (140 mg, 0.47 mmol) in dioxane (10 mL). The suspension was degassed and filled with nitrogen several times, and then dicyclohexyl-methylamine (3 mL, 14 mmol) was added under nitrogen. The mixture was stirred at room temperature for 10 min and then acrylic acid methyl ester (2.1 mL, 23 mmol) and water (0.21 mL, 12 mmol) was added. It was then heated via microwave at 100°C for 12 min. The crude product mixture was purified via flash column chromatography directly (EtOAc:hexanes, 10:90 to 100:0) to provide yellow syrup product (4.2 g, 83% yield). ^1H NMR (400 MHz, CD_3OD) δ 7.47 (d, J = 15.7 Hz, 1 H), 7.32 (d, J = 7.8 Hz, 2 H), 7.26–7.18 (m, 4 H), 7.03 (t, J = 7.3 Hz, 1 H), 6.93 (t, J = 7.3 Hz, 1 H), 6.45 (d, J = 15.7 Hz, 1 H), 4.02 (s, 2 H), 3.37 (s, 3 H), 3.34–3.32 (m, 2 H), 3.18 (t, J = 6.3 Hz, 2 H), 1.66 (s, 6 H), 1.40 (d, J = 6.3 Hz, 6 H). MS m/z 436.2 (MH^+).

(*E*)-*N*-Hydroxy-3-[4-[(2-[2-(1-hydroxy-1-methyl-ethyl)-1*H*-indol-3-yl]-ethyl)-isopropyl-amino)-methyl]-phenyl]-acrylamide (**11r**). Following method A, the title compound (45 mg, 32% yield) was prepared from **16** (140 mg, 0.32 mmol). ^1H NMR (400 MHz, $\text{DMSO}-d_6$) δ 10.74 (s, 1 H), 10.36 (s, 1 H), 9.03 (br, 1 H), 7.54–7.42 (m, 5 H), 7.26 (d, J = 8.1 Hz, 1 H), 7.10 (d, J = 7.8 Hz, 1 H), 6.93 (t, J = 7.4 Hz, 1 H), 6.81 (t, J = 7.3 Hz, 1 H), 5.24 (s, 1 H), 3.65 (s, 2 H), 3.34–3.31 (m, 2 H), 3.04–3.00 (m, 1 H), 2.87–2.83 (m, 2 H), 1.45 (s, 6 H), 1.04 (d, J = 6.0 Hz, 6 H). ^{13}C NMR (400 MHz, CD_3OD) δ 166.44, 142.7, 142.36, 141.25, 136.21, 135.05, 130.91, 130.42, 128.66, 121.95, 119.56, 118.78, 118.24, 112.06, 108.12, 71.18, 58.41, 55.53, 52.41, 52.12, 31.44, 25.78, 18.49, 18.43. MS m/z 436 (MH^+). HRMS calcd for $\text{C}_{26}\text{H}_{34}\text{N}_3\text{O}_3$ (MH^+) 436.2600, found 436.2607.

2-*tert*-Butyl-1*H*-pyrrolo[3,2-*b*]pyridine (**17f**). To an ice-cold solution of 3-methyl-pyridin-2-ylamine (25 g, 0.23 mol) in toluene (500 mL) under N_2 atmosphere was added potassium carbonate (32.0 g, 0.23 mol). The mixture was stirred at room temperature for 30 min, followed by dropwise addition of trimethylacetyl chloride (31.3 mL, 0.25 mol). The mixture was stirred at 25°C for 16 h and filtered. The precipitate was washed EtOAc. The combined filtrates were washed with aqueous NH_4Cl and brine. The organic layer was dried (MgSO_4) and concentrated to give 2,2-dimethyl-*N*-(3-methyl-pyridin-2-yl)-propionamide (21.3 g, 0.11 mol, 48% yield) as an off-white solid. To a cold suspension (-20°C) of this solid (21.3 g, 0.11 mol) in THF (300 mL) under N_2 was slowly added butyllithium (10 M in hexane, 33 mL, 0.33 mol), and the flask was allowed to warm up to room temperature and stand for 16 h. The mixture was then cooled below 0°C and quenched with 25 mL of aqueous 1N HCl, diluted with ether, and the layers were separated. The organic layer was washed with aqueous NaHCO_3 . The aqueous washings were extracted with additional ether, and the combined organic layers were washed with brine, dried (MgSO_4), and concentrated to give the title compound (22.7 g) as a crude white solid that was used directly in the next step without additional purification. ^1H NMR (CDCl_3) δ 8.25 (d, J = 4.4 Hz, 1H), 7.87 (br s, 1H), 7.56 (d, J = 6.9 Hz, 1H), 7.11 (dd, J = 4.8, 7.2 Hz, 1H), 2.23 (s, 3H), 1.35 (s, 9H). m/z 193.06 (MH^+).

Dimethyl-(1*H*-pyrrolo[3,2-*b*]pyridin-3-ylmethyl)-amine (**18a**). The title compound (1.1 g, >99% yield) was prepared according to method C from 1*H*-pyrrolo[3,2-*b*]pyridine (750 mg, 6.4 mmol). ^1H NMR (400 MHz, CD_3OD) δ 8.45 (d, J = 4.4 Hz, 1 H), 7.93 (dd, J = 8.4, 1.6 Hz, 1 H), 7.85 (s, 1 H), 7.29 (dd, J = 8.2, 4.8 Hz, 1 H), 4.46 (s, 2 H), 2.81 (s, 6 H). MS m/z 176.1 (MH^+).

Dimethyl-(1*H*-pyrrolo[3,2-*c*]pyridin-3-ylmethyl)-amine (**18d**). The title compound (2.6 g, 68% yield) was prepared according to method C from 1*H*-pyrrolo[3,2-*c*]pyridine (2.6 g, 22 mmol). ^1H NMR (400 MHz, CD_3OD) δ 9.13 (s, 1 H), 8.23 (d, J = 6.3 Hz, 1 H), 7.77 (s, 1 H), 7.56 (d, J = 6.4 Hz, 1 H), 4.50 (s, 2 H), 2.82 (s, 6 H). MS m/z 176.2 (MH^+).

(2-*tert*-Butyl-1*H*-pyrrolo[3,2-*b*]pyridin-3-ylmethyl)-dimethyl-amine (**18f**). In a dry vial was taken paraformaldehyde (517 mg, 17.2 mmol) in

dimethylacetamide:*n*-butanol (29:1 v/v, 3 mL) and subjected to microwave irradiation (100 °C for 13 min). Dimethylamine hydrochloride (1.4 g, 17.2 mmol) was added, and the mixture was heated and sonicated. To the resulting clear solution was added **17f** (2.0 g, 11.5 mmol), and the mixture was subjected to microwave irradiation (100 °C for 20 min). The mixture was diluted with MeOH and concentrated in vacuo. The residue was dissolved in DCM and washed with a small volume of aqueous Na₂CO₃. The aqueous washings were rewashed (2×) with DCM, and the combined organic layers were dried (MgSO₄), concentrated, and dried to give the title compound (2.31 g, 9.99 mmol, 87% yield) as a yellow solid. ¹H NMR (CDCl₃) δ 9.4 (br s, 1H), 8.21 (dd, *J* = 1.4, 4.8 Hz, 1H), 7.99 (d, *J* = 7.9 Hz, 1H), 7.02 (dd, *J* = 4.8, 7.9 Hz, 1H), 3.63 (s, 2H), 2.23 (s, 6H), 1.53 (s, 9H). *m/z* 232.0 (MH⁺).

Imidazo[1,2-*a*]pyridin-3-ylmethyl-dimethyl-amine (18g). The title compound (900 mg, 68% yield) was prepared according to method C from imidazo[1,2-*a*]pyridine (880 mg, 7.5 mmol). ¹H NMR (400 MHz, CDCl₃) δ 8.19 (d, *J* = 6.8 Hz, 1 H), 7.60 (d, *J* = 9.4 Hz, 1 H), 7.53 (s, 1 H), 7.22 (ddd, *J* = 9.2, 6.7, 1.3 Hz, 1 H), 6.84 (t, *J* = 6.7 Hz, 1 H), 4.78 (s, 2 H), 3.60 (s, 6 H). MS *m/z* 176.1 (MH⁺).

(1H-Pyrrolo[3,2-*b*]pyridin-3-yl)-acetonitrile (19a). The title compound (340 mg, 34% yield) was prepared according to method D from **18a** (1.1 g, 6.3 mmol). MS *m/z* 158.1 (MH⁺).

1H-Pyrrolo[3,2-*c*]pyridin-3-yl)-acetonitrile (19d). The title compound (600 mg, 26% yield) was prepared according to method D from **18d** (2.6 g, 15 mmol).

(2-*tert*-Butyl-1H-pyrrolo[2,3-*b*]pyridin-3-yl)-acetonitrile (19f). To a solution of **18f** (2.0 g, 8.66 mmol) in THF (40 mL) was slowly added dimethyl sulfate (900 μL, 9.51 mmol), and the mixture was refluxed for 30 min. The solvent was removed in vacuo, and the residue was suspended in 30 mL water to which NaCN (0.57 g, 11.2 mmol) was added. After refluxing for 1 h, the aqueous suspension was washed with excess EtOAc (3×), and the combined organic layers were dried (MgSO₄) and concentrated to give a residue that was purified by flash column (0–40% EtOAc in Hex) to give the title compound (0.33 g, 1.55 mmol, 18% yield) as a white solid. ¹H NMR (CDCl₃) δ 9.87 (br s, 1H), 8.31 (dd, *J* = 1.4, 4.9 Hz, 1H), 7.92 (d, *J* = 7.4 Hz, 1H), 7.12 (dd, *J* = 4.9, 8.1 Hz, 1H), 3.95 (s, 2H), 1.56 (s, 9H). *m/z* 214.1 (MH⁺).

Imidazo[1,2-*a*]pyridin-3-yl-acetonitrile (19g). The title compound (110 mg, 5.1% yield) was prepared according to method D from **18g** (2.6 g, 15 mmol). MS *m/z* 158.0 (MH⁺).

2-(1H-Pyrrolo[3,2-*b*]pyridin-3-yl)-ethylamine (20a). The title compound (340 mg, 98% yield) was prepared according to same procedure as **13m** from **19a** (340 mg, 2.2 mmol). MS *m/z* 162.1 (MH⁺).

2-(6-Methyl-7H-pyrrolo[2,3-*d*]pyrimidin-5-yl)-ethylamine (20b). The title compound (140 mg, 72% yield) was prepared according to same procedure as **13m** from (6-methyl-7H-pyrrolo[2,3-*d*]pyrimidin-5-yl)-acetonitrile (200 mg, 1.1 mmol). ¹H NMR (400 MHz, DMSO-*d*₆) δ 8.81 (s, 1 H), 8.60 (s, 1 H), 2.77–2.75 (m, 4 H), 2.30 (s, 3 H). MS *m/z* 177.1 (MH⁺).

2-(6-Methyl-5H-pyrrolo[2,3-*b*]pyrazin-7-yl)-ethylamine (20c). The title compound (200 mg, 98% yield) was prepared according to same procedure as **13m** from (6-methyl-5H-pyrrolo[2,3-*b*]pyrazin-7-yl)-acetonitrile (200 mg, 1.1 mmol). MS *m/z* 177.1 (MH⁺).

2-(1H-Pyrrolo[3,2-*c*]pyridin-3-yl)-ethylamine (20d). Rhodium on alumina (200 mg, 0.1 mmol) was added to a solution of **19d** (200 mg, 1.3 mmol) in ammonium hydroxide (6 mL) and ethanol (12 mL). The mixture was stirred under hydrogen atmosphere (50 psi) in a Parr shaker overnight. Upon completion of the reaction, the solution was filtered and evaporated off. The resulting product (200 mg, 98% yield) was used directly in the next step.

2-(2-*tert*-Butyl-1H-pyrrolo[2,3-*b*]pyridin-3-yl)-ethylamine (20f). The title compound (524 mg, 2.03 mmol, 86% yield, 84% purity) was prepared according to same procedure as **13m** from **19f** (500 mg, 2.34 mmol) and was directly used in the next step. *m/z* 218.2 (MH⁺).

2-Imidazo[1,2-*a*]pyridin-3-yl-ethylamine (20g). The title compound (140 mg, 79% yield) was prepared according to same procedure as **20d** from **20g** (180 mg, 1.1 mmol). ¹H NMR (400 MHz, CD₃OD) δ 8.32 (d, *J* = 6.9 Hz, 1 H), 7.56 (d, *J* = 8.9 Hz, 1 H), 7.44 (s, 1 H), 7.32 (ddd, *J* = 9.1, 6.8, 1.2 Hz, 1 H), 6.99 (t, *J* = 6.8 Hz, 1 H), 3.12 (t, *J* = 6.8 Hz, 2 H), 3.05 (t, *J* = 6.8 Hz, 2 H). MS *m/z* 162.1 (MH⁺).

Typical Procedure for the Formation of 2-Ylpyrazolo[1,5-*a*]pyridine-3-carboxylic Acid Ethyl Esters. To a solution of amino-pyridinium iodide (22 g, 99 mmol) and anhydrous potassium carbonate (17.8 g, 128.7 mmol) in dimethylformamide (225 mL) was added an alkyl- or aryl-2-pentynoate (198 mmol). The solution was stirred at room temperature for 24 h. The reaction mixture was poured into 1.2 L of ice water. The resulting light-brown precipitate was collected by vacuum filtration and air-dried overnight to yield 11.9 g (55% yield) of crude product, which was used without further purification.

2-Methyl-pyrazolo[1,5-*a*]pyridine-3-carboxylic Acid Ethyl Ester (21i). The title compound (6.2 g, 52% yield) was prepared according to the above procedure from amino-pyridinium iodide (13.0 g, 58.5 mmol) and methyl-2-butynoate (13.6 mL, 117 mmol). ¹H NMR (400 MHz, CDCl₃) δ 8.42–8.39 (m, 1 H), 8.09–8.06 (m, 1 H), 7.37–7.33 (m, 1 H), 6.89–6.86 (m, 1 H), 4.39 (q, *J* = 7.9 Hz, 2 H), 2.68 (s, 3 H), 1.43 (t, *J* = 9.0 Hz, 3 H). MS *m/z* 205 (MH⁺).

2-Ethyl-pyrazolo[1,5-*a*]pyridine-3-carboxylic Acid Ethyl Ester (21j). The title compound (11 g, 55% yield) was prepared according to the above procedure from amino-pyridinium iodide (22 g, 99 mmol) and ethyl-2-butynoate (24.98 mL, 198 mmol). ¹H NMR (400 MHz, CDCl₃) δ 8.43 (ddd, *J* = 6.9, 1.1, 1.1 Hz, 1 H), 8.10 (ddd, *J* = 8.8, 1.2, 1.3 Hz, 1 H), 7.35 (ddd, *J* = 9.0, 6.8, 1.2 Hz, 1 H), 6.88 (ddd, *J* = 7.7, 6.1, 0.7 Hz, 1 H), 4.39 (q, *J* = 7.1 Hz, 2 H), 3.13 (q, *J* = 7.5 Hz, 2 H), 1.43 (t, *J* = 7.0 Hz, 3 H), 1.36 (t, *J* = 7.8 Hz, 3 H). MS *m/z* 219 (MH⁺).

2-Phenyl-pyrazolo[1,5-*a*]pyridine-3-carboxylic Acid Ethyl Ester (21k). The title compound (20 g, 74% yield) was prepared according to the above procedure from amino-pyridinium iodide (13.0 g, 58.5 mmol) and phenyl-propynoic acid ethyl ester (19.3 mL, 117 mmol). ¹H NMR (400 MHz, CDCl₃) δ 8.52 (ddd, *J* = 7.0, 1.2, 1.2 Hz, 1 H), 8.21 (ddd, *J* = 8.9, 1.2, 1.2 Hz, 1 H), 7.80–7.77 (m, 2 H), 7.48–7.38 (m, 3 H), 6.95 (ddd, *J* = 7.7, 6.2, 0.8 Hz, 1 H), 4.32 (q, *J* = 7.2 Hz, 2 H), 1.31 (t, *J* = 7.1 Hz, 3 H). MS *m/z* 267 (MH⁺).

Typical Procedure for the Formation of 2-Ylpyrazolo[1,5-*a*]pyridine-3-carbaldehydes. A solution of pyrazolo[1,5-*a*]pyridine-3-carboxylic acid ethyl ester (68.7 mmol) in THF (300 mL) was cooled in an ice bath, and lithium aluminum hydride (2.6 g, 68.7 mmol) was added. The reaction mixture was stirred at room temperature overnight. Water was added until bubbling stopped. Silica gel was added, and the solvent was evaporated in vacuo. The resulting residue was purified via silica gel chromatography eluted with 20% EtOAc:hexanes to 100% to yield 9.67 g (80% yield) of product as a yellow–brown oil.

To a solution of (pyrazolo[1,5-*a*]pyridin-3-yl)-methanol (54.9 mmol) in THF (500 mL) was added MnO₂ (23.88 g, 274.5 mmol, Aldrich cat. no. 217646, 85%, dried overnight in oven at 120 °C) and stirred at reflux for 1.5 h. The reaction mixture was filtered through Celite and concentrated under reduced pressure to give 9.4 g (98% yield) of product, which was used without further purification.

2-Methyl-pyrazolo[1,5-*a*]pyridine-3-carbaldehyde (22i). (2-Methyl-pyrazolo[1,5-*a*]pyridin-3-yl)-methanol (3.9 g, 80% yield) was prepared according to same procedure as above from **21i** (6.1 g, 30 mmol). ¹H NMR (400 MHz, CDCl₃) δ 8.28 (dt, *J* = 7.0, 1.0 Hz, 1 H), 7.47 (dt, *J* = 9.0, 1.2 Hz, 1 H), 7.06 (ddd, *J* = 8.9, 6.8, 1.1 Hz, 1 H), 6.65 (td, *J* = 6.9, 1.6 Hz, 1 H), 4.78 (s, 2 H), 2.43 (s, 3 H). MS *m/z* 163.1 (MH⁺).

The title compound (3.8 g, 97% yield) was prepared according to same procedure as above from (2-methyl-pyrazolo[1,5-*a*]pyridin-3-yl)-methanol (3.9 g, 24 mmol). ¹H NMR (400 MHz, CDCl₃) δ 10.02 (s, 1 H), 8.40 (dt, *J* = 6.8, 1.0 Hz, 1 H), 8.14 (dt, *J* = 8.7, 1.3 Hz, 1 H), 7.42

(ddd, $J = 8.7, 7.0, 1.1$ Hz, 1 H), 6.93 (ddd, $J = 7.7, 6.2, 0.8$ Hz, 1 H), 2.62 (s, 3 H). MS m/z 161.1 (MH^+).

2-Ethyl-pyrazolo[1,5-*a*]pyridine-3-carbaldehyde (22j). (2-Ethyl-pyrazolo[1,5-*a*]pyridin-3-yl)-methanol (9.67 g 80% yield) was prepared according to same procedure as above from **22i** (15 g, 68.7 mmol) 1H NMR (400 MHz, $CDCl_3$) δ 8.35 (dt, $J = 8.3, 1.3$ Hz, 1 H), 7.51 (dt, $J = 8.9, 1.3$ Hz, 1 H), 7.09 (ddd, $J = 9.1, 6.5, 1.2$ Hz, 1 H), 6.68 (ddd, $J = 7.5, 6.2, 0.6$ Hz, 1 H), 4.83 (s, 2 H), 2.79 (q, $J = 7.5$ Hz, 2 H), 1.28 (t, $J = 7.6$ Hz, 3 H). MS m/z 177.1 (MH^+).

The title compound (9.4 g 98% yield) was prepared according to same procedure as above from (2-ethyl-pyrazolo[1,5-*a*]pyridin-3-yl)-methanol (9.67 g, 54.9 mmol). 1H NMR (400 MHz, $CDCl_3$) δ 10.04 (s, 1 H), 8.41 (dt, $J = 6.8, 1.3$ Hz, 1 H), 8.15 (dt, $J = 8.9, 1.5$ Hz, 1 H), 7.41 (ddd, $J = 8.8, 6.8, 1.1$ Hz, 1 H), 6.93 (ddd, $J = 7.8, 6.1, 0.8$ Hz, 1 H), 3.03 (q, $J = 7.6$ Hz, 2 H), 1.35 (t, $J = 7.5$ Hz, 3 H). MS m/z 175.1 (MH^+).

2-Phenyl-pyrazolo[1,5-*a*]pyridine-3-carbaldehyde (22k). (2-Phenyl-pyrazolo[1,5-*a*]pyridin-3-yl)-methanol (3.6 g, 43% yield) was prepared according to same procedure as above from **21k** (10 g, 38 mmol). 1H NMR (400 MHz, $CDCl_3$) δ 8.49 (dt, $J = 7.0, 1.1$ Hz, 1 H), 7.91 (dt, $J = 6.7, 1.6$ Hz, 2 H), 7.65 (dt, $J = 8.9, 1.1$ Hz, 1 H), 7.54–7.49 (m, 2 H), 7.45 (dt, $J = 7.2, 1.9$ Hz, 1 H), 7.19 (ddd, $J = 8.9, 6.7, 1.1$ Hz, 1 H), 6.81 (ddd, $J = 7.5, 6.2, 0.8$ Hz, 1 H), 4.96 (s, 2 H). MS m/z 225.0 (MH^+).

The title compound (870 mg, 98% yield) was prepared according to same procedure as above from (2-phenyl-pyrazolo[1,5-*a*]pyridin-3-yl)-methanol (900 mg, 4.0 mmol). 1H NMR (400 MHz, $CDCl_3$) δ 10.04 (s, 1 H), 8.53 (dt, $J = 6.9, 1.0$ Hz, 1 H), 8.36 (dt, $J = 8.8, 1.2$ Hz, 1 H), 7.73–7.70 (m, 2 H), 7.50–7.44 (m, 4 H), 7.03 (ddd, $J = 7.6, 6.3, 0.6$ Hz, 1 H). MS m/z 223.0 (MH^+).

Typical Procedure for the Formation of 2-yl-3-((*E*)-2-nitro-vinyl)-pyrazolo[1,5-*a*]pyridines. To a solution of 2-yl-pyrazolo[1,5-*a*]pyridine-3-carbaldehyde (48 mmol) in nitromethane (29 g, 480 mmol) was added ammonium acetate (18 g, 240 mmol) and heated at 100 °C for 1 h. The reaction mixture was concentrated under vacuum, and the resulting residue was chromatographed (silica gel, 10% EtOAc/hexane to 100% EtOAc/hexane) to obtain the title compound (62–83% yields).

2-Methyl-3-((*E*)-2-nitro-vinyl)-pyrazolo[1,5-*a*]pyridine (23i). The title compound (1 g, 83% yield) was prepared according to same procedure as above from **22i** (950 mg, 5.9 mmol). 1H NMR (400 MHz, $CDCl_3$) δ 8.50 (dt, $J = 6.9, 1.1$ Hz, 1 H), 8.31 (d, $J = 13.6$ Hz, 1 H), 7.70 (dt, $J = 8.8, 1.0$ Hz, 1 H), 7.58 (d, $J = 13.7$ Hz, 1 H), 7.49 (ddd, $J = 8.8, 6.9, 1.2$ Hz, 1 H), 7.00 (ddd, $J = 7.6, 6.1, 0.6$ Hz, 1 H), 2.62 (s, 3 H). MS m/z 204.0 (MH^+).

2-Ethyl-3-((*E*)-2-nitro-vinyl)-pyrazolo[1,5-*a*]pyridine (23j). The title compound (6.3 g, 62% yield) was prepared according to same procedure as above from **22j** (8.3 g, 48 mmol). 1H NMR (400 MHz, $CDCl_3$) δ 8.52 (dt, $J = 6.9, 1.0$ Hz, 1 H), 8.31 (d, $J = 13.6$ Hz, 1 H), 7.70 (dt, $J = 8.9, 1.2$ Hz, 1 H), 7.58 (d, $J = 13.5$ Hz, 1 H), 7.49 (ddd, $J = 8.7, 6.9, 1.1$ Hz, 1 H), 7.01 (ddd, $J = 7.6, 6.2, 0.7$ Hz, 1 H), 2.99 (q, $J = 7.4$ Hz, 2 H), 1.42 (t, $J = 7.6$ Hz, 3 H). MS m/z 218.0 (MH^+).

3-((*E*)-2-Nitro-vinyl)-2-phenyl-pyrazolo[1,5-*a*]pyridine (23k). The title compound (1 g, 99% yield) was prepared according to same procedure as above from **22k** (850 mg, 3.8 mmol) 1H NMR (400 MHz, $CDCl_3$) δ 8.55 (dt, $J = 6.9, 1.1$ Hz, 1 H), 8.26 (d, $J = 13.5$ Hz, 1 H), 7.72 (dt, $J = 8.8, 1.2$ Hz, 1 H), 7.61–7.58 (m, 2 H), 7.53 (d, $J = 13.7$ Hz, 1 H), 7.50–7.44 (m, 4 H), 7.01 (ddd, $J = 7.6, 6.3, 0.7$ Hz, 1 H). MS m/z 265.9 (MH^+).

Typical Procedure for the Formation of 2-yl-pyrazolo[1,5-*a*]pyridin-3-yl Ethylamines. To a solution of 2-yl-3-((*E*)-2-nitro-vinyl)-pyrazolo[1,5-*a*]pyridine (31 mmol) in THF (300 mL) was added BF_3 (93 mL, 1 M in THF) and BH_3 (188 mL, 1 M in THF) and stirred at 65 °C overnight. The reaction was quenched with MeOH until bubbling ceased. The solution was concentrated in vacuo, and aqueous NaOH (1N) was added followed by extraction with CH_2Cl_2 :EtOH (4:1) several times until no product was detected by TLC in the aqueous

solution. The organic layer was washed with brine. The brine layer was further extracted with CH_2Cl_2 :EtOH (4:1) several times until no product was detected by TLC in brine layer. The organic layers were combined, concentrated under vacuum, and purified on a short silica gel column, eluting with CH_2Cl_2 to 25% MeOH/ CH_2Cl_2 with 1% NH_4OH , (82.5–95% yield).

2-(2-Methyl-pyrazolo[1,5-*a*]pyridin-3-yl)-ethylamine (24i). The title compound (820 mg, 95% yield) was prepared according to same procedure as above from **23i** (1.0 g, 4.9 mmol). 1H NMR (400 MHz, CD_3OD) δ 8.69 (dt, $J = 7.0, 0.9$ Hz, 1 H), 8.00 (dt, $J = 9.1, 1.2$ Hz, 1 H), 7.76 (ddd, $J = 9.0, 7.1, 1.0$ Hz, 1 H), 7.40 (ddd, $J = 7.7, 6.3, 0.6$ Hz, 1 H), 3.36–3.31 (m, 2 H), 3.23–3.18 (m, 2 H), 2.61 (s, 3 H). MS m/z 176.1 (MH^+).

2-(2-Ethyl-pyrazolo[1,5-*a*]pyridin-3-yl)-ethylamine (24j). The title compound (5.75 g, 85% pure, 82.5% yield) was prepared according to same procedure as above from **23i** (6.8 g, 31 mmol) and used in the next step without further purification. 1H NMR (400 MHz, CD_3OD) δ 8.43 (dt, $J = 7.1, 1.1$ Hz, 1 H), 7.60 (dt, $J = 8.8, 1.3$ Hz, 1 H), 7.24 (ddd, $J = 8.9, 6.8, 1.0$ Hz, 1 H), 6.86 (ddd, $J = 7.6, 6.0, 0.7$ Hz, 1 H), 7.33 (ddd, $J = 9.1, 6.8, 1.1$ Hz, 1 H), 3.14–3.09 (m, 2 H), 2.86 (q, $J = 7.4$ Hz, 2 H), 1.36 (t, $J = 7.8$ Hz, 3 H). MS m/z 190.1 (MH^+).

2-(2-Phenyl-pyrazolo[1,5-*a*]pyridin-3-yl)-ethylamine (24k). The title compound (700 mg, 78% yield) was prepared according to same procedure as above from **23k** (1.0 g, 3.8 mmol). 1H NMR (400 MHz, CD_3OD) δ 8.55 (dt, $J = 7.1, 1.1$ Hz, 1 H), 7.76–7.70 (m, 3 H), 7.57–7.53 (m, 2 H), 7.49 (tt, $J = 7.3, 1.8$ Hz, 1 H), 7.33 (ddd, $J = 9.1, 6.8, 1.1$ Hz, 1 H), 6.97 (ddd, $J = 7.5, 6.2, 0.7$ Hz, 1 H), 3.30 (t, $J = 8.7$ Hz, 2 H), 3.09 (t, $J = 8.0$ Hz, 2 H). MS m/z 238.0 (MH^+).

(*E*)-N-Hydroxy-3-(4-{[2-(1H-pyrrolo[3,2-*b*]pyridin-3-yl)-ethylamino]-methyl}-phenyl)-acrylamide (25a). Following method A, (*E*)-3-(4-{[2-(1H-pyrrolo[3,2-*b*]pyridin-3-yl)-ethylamino]-methyl}-phenyl)-acrylic acid methyl ester (200 mg, 48% yield) was prepared from **20a** (200 mg, 1.2 mmol). 1H NMR (400 MHz, CD_3OD) δ 8.27 (dd, $J = 4.7, 1.4$ Hz, 1 H), 7.86 (dd, $J = 8.2, 1.4$ Hz, 1 H), 7.75 (s, 1 H), 7.72–7.69 (m, 2 H), 7.56 (d, $J = 8.3$ Hz, 2 H), 7.51 (s, 1 H), 7.22 (dd, $J = 8.1, 4.7$ Hz, 1 H), 6.61 (d, $J = 15.9$ Hz, 1 H), 4.24 (s, 2 H), 3.81 (s, 3 H), 3.33 (t, $J = 6.1$ Hz, 2 H), 3.22 (t, $J = 6.5$ Hz, 2 H). MS m/z 336.2 (MH^+).

The title compound (10 mg, 5.5% yield) was prepared according to method B from (*E*)-3-(4-{[2-(1H-pyrrolo[3,2-*b*]pyridin-3-yl)-ethylamino]-methyl}-phenyl)-acrylic acid methyl ester (190 mg, 0.54 mmol). 1H NMR (400 MHz, CD_3OD) δ 8.28 (dd, $J = 4.7, 1.4$ Hz, 1 H), 7.80 (dd, $J = 8.3, 1.4$ Hz, 1 H), 7.55 (d, $J = 16.0$ Hz, 1 H), 7.51 (d, $J = 8.3$ Hz, 2 H), 7.43 (s, 1 H), 7.35 (d, $J = 8.6$ Hz, 2 H), 7.17 (dd, $J = 8.3, 4.9$ Hz, 1 H), 6.46 (d, $J = 16.3$ Hz, 1 H), 3.87 (s, 2 H), 3.10 (t, $J = 6.8$ Hz, 2 H), 3.01 (t, $J = 6.7$ Hz, 2 H). MS m/z 336.9 (MH^+). HRMS calcd for $C_{19}H_{20}N_4O_2$ (M^+) 335.1508, found 335.1518.

(*E*)-N-Hydroxy-3-(4-{[2-(6-methyl-7H-pyrrolo[2,3-*d*]pyrimidin-5-yl)-ethylamino]-methyl}-phenyl)-acrylamide (25b). Following method A, (*E*)-3-(4-{[2-(6-methyl-7H-pyrrolo[2,3-*d*]pyrimidin-5-yl)-ethylamino]-methyl}-phenyl)-acrylic acid methyl ester (60 mg, 21% yield) was prepared from **20b** (140 mg, 0.80 mmol). 1H NMR (400 MHz, CD_3OD) δ 8.76 (s, 1 H), 8.61 (s, 1 H), 7.68 (d, $J = 16.2$ Hz, 1 H), 7.55 (d, $J = 8.3$ Hz, 2 H), 7.35 (d, $J = 8.4$ Hz, 2 H), 6.52 (d, $J = 15.8$ Hz, 1 H), 3.82 (s, 2 H), 3.80 (s, 3 H), 2.96 (t, $J = 7.6$ Hz, 2 H), 2.85 (t, $J = 7.5$ Hz, 2 H), 2.43 (s, 3 H). MS m/z 351.1 (MH^+).

The title compound (4 mg, 7% yield) was prepared according to method B from (*E*)-3-(4-{[2-(6-methyl-7H-pyrrolo[2,3-*d*]pyrimidin-5-yl)-ethylamino]-methyl}-phenyl)-acrylic acid methyl ester (60 mg, 0.17 mmol). 1H NMR (400 MHz, $DMSO-d_6$) δ 8.81 (s, 1 H), 8.60 (s, 1 H), 7.48 (d, $J = 8.2$ Hz, 2 H), 7.42 (d, $J = 15.9$ Hz, 1 H), 7.33 (d, $J = 7.8$ Hz, 2 H), 6.43 (d, $J = 16.1$ Hz, 1 H), 3.75 (s, 2 H), 2.83 (t, $J = 6.6$ Hz, 2 H), 2.73 (t, $J = 7.0$ Hz, 2 H), 2.34 (s, 3 H). MS m/z 351.8 (MH^+). HRMS calcd for $C_{19}H_{21}N_5O_2$ (MH^+) 352.1774, found 352.1784.

(*E*)-N-Hydroxy-3-(4-{[2-(6-methyl-5H-pyrrolo[2,3-*b*]pyrazin-7-yl)-ethylamino]-methyl}-phenyl)-acrylamide (25c). Following method A,

(E)-3-(4-{[2-(6-methyl-5H-pyrrolo[2,3-b]pyrazin-7-yl)-ethylamino]-methyl}-phenyl)-acrylic acid methyl ester (130 mg, 41% yield) was prepared from **20c** (160 mg, 0.91 mmol). ¹H NMR (400 MHz, CD₃OD) δ 8.76 (s, 1 H), 8.61 (s, 1 H), 7.68 (d, *J* = 16.2 Hz, 1 H), 7.54 (d, *J* = 7.9 Hz, 2 H), 7.34 (d, *J* = 8.1 Hz, 2 H), 6.51 (d, *J* = 16.0 Hz, 1 H), 3.82 (s, 2 H), 3.80 (s, 3 H), 2.96 (t, *J* = 7.3 Hz, 2 H), 2.85 (t, *J* = 7.1 Hz, 2 H), 2.42 (s, 3 H). MS *m/z* 350.8 (MH⁺).

The title compound (33 mg, 25% yield) was prepared according to method B from (E)-3-(4-{[2-(6-methyl-5H-pyrrolo[2,3-b]pyrazin-7-yl)-ethylamino]-methyl}-phenyl)-acrylic acid methyl ester (130 mg, 0.37 mmol). ¹H NMR (400 MHz, DMSO-*d*₆) δ 8.80 (s, 1 H), 8.60 (s, 1 H), 7.47 (d, *J* = 8.1 Hz, 2 H), 7.42 (d, *J* = 15.2 Hz, 1 H), 7.33 (d, *J* = 8.7 Hz, 2 H), 6.42 (d, *J* = 15.5 Hz, 1 H), 3.74 (s, 2 H), 2.82 (t, *J* = 6.7 Hz, 2 H), 2.71 (t, *J* = 7.2 Hz, 2 H), 2.33 (s, 3 H). ¹³C NMR (400 MHz, CD₃OD) δ 166.35, 152.32, 150.57, 146.53, 141.23, 136.83, 135.35, 130.18, 128.96, 128.28, 120.93, 118.36, 108.64, 53.75, 50.03, 24.51, 11.30. MS *m/z* 351.7 (MH⁺). HRMS calcd for C₁₉H₂₁N₅O₂ (MH⁺) 352.1774, found 352.1775.

(E)-N-Hydroxy-3-(4-{[2-(1H-pyrrolo[3,2-c]pyridin-3-yl)-ethylamino]-methyl}-phenyl)-acrylamide (**25d**). Following method A, (E)-3-(4-{[2-(1H-pyrrolo[3,2-c]pyridin-3-yl)-ethylamino]-methyl}-phenyl)-acrylic acid methyl ester (270 mg, 65% yield) was prepared from **20d** (200 mg, 1.2 mmol). ¹H NMR (400 MHz, CD₃OD) δ 8.80 (s, 1 H), 8.14 (d, *J* = 6.2 Hz, 1 H), 7.68 (d, *J* = 16.1 Hz, 1 H), 7.58 (d, *J* = 7.9 Hz, 2 H), 7.43–7.39 (m, 3 H), 7.27 (s, 1 H), 6.53 (d, *J* = 16.2 Hz, 1 H), 3.96 (s, 2 H), 3.80 (s, 3 H), 3.33–3.32 (m, 2 H), 2.13–2.06 (m, 2 H). MS *m/z* 336.1 (MH⁺).

The title compound (20 mg, 7.8% yield) was prepared according to method B from (E)-3-(4-{[2-(1H-pyrrolo[3,2-c]pyridin-3-yl)-ethylamino]-methyl}-phenyl)-acrylic acid methyl ester (270 mg, 0.77 mmol). ¹H NMR (400 MHz, DMSO-*d*₆) δ 8.79 (s, 1 H), 8.12 (d, *J* = 5.8 Hz, 1 H), 7.48 (d, *J* = 7.8 Hz, 2 H), 7.43 (d, *J* = 16.0 Hz, 1 H), 7.36 (d, *J* = 8.2 Hz, 2 H), 7.30 (dd, *J* = 5.6, 1.2 Hz, 1 H), 7.21 (s, 1 H), 6.43 (d, *J* = 17.2 Hz, 1 H), 3.77 (s, 2 H), 2.91 (t, *J* = 7.3 Hz, 2 H), 2.82 (t, *J* = 7.0 Hz, 2 H). ¹³C NMR (400 MHz, CD₃OD) δ 166.33, 142.06, 141.99, 141.91, 141.19, 140.12, 135.33, 130.18, 128.95, 125.76, 125.63, 118.34, 114.21, 108.25, 53.72, 50.19, 25.68. MS *m/z* 337 (MH⁺). HRMS calcd for C₁₉H₂₀N₄O₂ (MH⁺) 337.1665, found 337.1657.

(E)-3-(4-{[2-(2-*tert*-butyl-1H-pyrrolo[2,3-b]pyridin-3-yl)-ethylamino]-methyl}-phenyl)-N-hydroxy-acrylamide (**25f**). Following method A, **20f** (524 mg, 2.03 mmol, approximately 84% pure) was converted into (E)-3-(4-{[2-(2-*tert*-butyl-1H-pyrrolo[2,3-b]pyridin-3-yl)-ethylamino]-methyl}-phenyl)-acrylic acid methyl ester (392 mg, 1.0 mmol, 49% yield). ¹H NMR (DMSO-*d*₆) δ 10.99 (br s, 1H), 8.09 (dd, *J* = 1.5, 5.0 Hz, 1H), 7.77 (d, *J* = 7.8 Hz, 1H), 7.66 (m, 3H), 7.40 (d, *J* = 7.9 Hz, 2H), 6.95 (dd, *J* = 4.8, 7.8 Hz, 1H), 6.61 (d, *J* = 15.6 Hz, 1H), 3.83 (s, 2H), 3.73 (s, 3H), 2.99 (m, 2H), 2.73 (m, 2H), 1.40 (s, 9H). *m/z* 392.0 (MH⁺).

Following method B, (E)-3-(4-{[2-(2-*tert*-butyl-1H-pyrrolo[2,3-b]pyridin-3-yl)-ethylamino]-methyl}-phenyl)-acrylic acid methyl ester (400 mg, 1.02 mmol) was converted to **25f** (52 mg, 0.13 mmol, 13% yield) after HPLC purification. ¹H NMR (CD₃OD) δ 8.07 (d, *J* = 4.7 Hz, 1H), 7.82 (d, *J* = 8.0 Hz, 1H), 7.51 (m, 3H), 7.35 (d, *J* = 8.8 Hz, 2H), 6.99 (dd, *J* = 5.0, 8.0 Hz, 1H), 6.47 (d, *J* = 15.9 Hz, 1H), 3.82 (s, 2H), 3.09 (m, 2H), 2.80 (m, 2H), 1.46 (s, 9H). ¹³C NMR (CD₃OD) δ 166.0, 148.3, 146.1, 142.7, 140.7, 136.9, 131.1, 129.4, 127.2, 123.5, 119.5, 116.4, 104.6, 52.5, 34.7, 31.1, 24.1. *m/z* 393.2 (MH⁺). HRMS (MH⁺) calcd for C₂₃H₂₈N₄O₂, 393.2291, found 393.2291.

(E)-N-Hydroxy-3-{4-[(2-imidazo[1,2-*a*]pyridin-3-yl)-ethylamino]-methyl}-phenyl)-acrylamide (**25g**). (E)-3-{4-[(2-imidazo[1,2-*a*]pyridin-3-yl)-ethylamino]-methyl}-phenyl)-acrylic acid methyl ester (50 mg, 17% yield) was prepared according to general method A from **20g** (140 mg, 0.87 mmol). MS *m/z* 335.7 (MH⁺).

The title compound (13 mg, 26% yield) was prepared according to general procedure method B from (E)-3-{4-[(2-imidazo[1,2-*a*]pyridin-

3-yl)-ethylamino]-methyl}-phenyl)-acrylic acid methyl ester (50 mg, 0.15 mmol). ¹H NMR (400 MHz, CD₃OD) δ 8.24 (d, *J* = 7.7 Hz, 1 H), 7.57–7.49 (m, 4 H), 7.39 (d, *J* = 14.4 Hz, 1 H), 7.36 (d, *J* = 8.0 Hz, 2 H), 7.30 (t, *J* = 7.8 Hz, 1 H), 6.96–6.92 (m, 1 H), 6.46 (d, *J* = 15.5 Hz, 1 H), 3.87 (s, 2 H), 3.17 (t, *J* = 7.7 Hz, 2 H), 3.01 (t, *J* = 7.4 Hz, 2 H). ¹³C NMR (400 MHz, CD₃OD) δ 166.30, 146.67, 141.44, 141.19, 135.53, 131.21, 130.31, 129.03, 126.09, 125.17, 123.60, 118.47, 117.70, 113.85, 53.61, 46.96, 24.27. MS *m/z* 336.7 (MH⁺). HRMS calcd for C₁₉H₂₀N₄O₂ (MH⁺) 337.1665, found 337.1652.

(E)-N-Hydroxy-3-(4-{[2-(2-methyl-pyrazolo[1,5-*a*]pyridin-3-yl)-ethylamino]-methyl}-phenyl)-acrylamide (**25i**). (E)-3-(4-{[2-(2-methyl-pyrazolo[1,5-*a*]pyridin-3-yl)-ethylamino]-methyl}-phenyl)-acrylic acid methyl ester (510 mg, 31% yield) was prepared according to general procedure method A from **24i** (820 mg, 4.7 mmol). ¹H NMR (400 MHz, CDCl₃) δ 8.28 (d, *J* = 6.7 Hz, 1 H), 7.53 (d, *J* = 16.6 Hz, 1 H), 7.44 (d, *J* = 7.2 Hz, 2 H), 7.40–7.37 (m, 3 H), 7.02 (dd, *J* = 8.9, 6.8 Hz, 1 H), 6.63 (t, *J* = 7.0 Hz, 1 H), 6.32 (d, *J* = 16.3 Hz, 1 H), 3.81 (s, 3 H), 3.70 (s, 2 H), 3.00–2.98 (m, 4 H), 2.39 (s, 3 H). MS *m/z* 349.9 (MH⁺).

The title compound (50 mg, 25% yield) was prepared according to method B from (E)-3-(4-{[2-(2-methyl-pyrazolo[1,5-*a*]pyridin-3-yl)-ethylamino]-methyl}-phenyl)-acrylic acid methyl ester (200 mg, 0.57 mmol). ¹H NMR (400 MHz, CD₃OD) δ 8.38 (d, *J* = 7.1, 1 H), 7.63 (d, *J* = 7.6 Hz, 2 H), 7.61 (d, *J* = 9.6, 1 H), 7.54 (dd, *J* = 13.1, 3.5 Hz, 1 H), 7.50 (d, *J* = 7.6, 2 H), 7.20 (dd, *J* = 7.6, 7.1 Hz, 1 H), 6.81 (t, *J* = 7.1 Hz, 1 H), 6.52 (d, *J* = 15.6 Hz, 1 H), 4.18 (s, 2 H), 3.12 (m, 4 H), 2.42 (s, 3 H). ¹³C NMR (400 MHz, CD₃OD) δ 166.2, 150.89, 141.00, 140.75, 140.05, 135.87, 130.52, 129.09, 128.83, 124.65, 118.72, 117.11, 112.69, 106.03, 53.31, 49.71, 22.90, 11.81. MS *m/z* 351.0 (MH⁺). HRMS calcd for C₁₂H₂₅N₄O₂ (MH⁺) 351.1821, found 351.1831.

(E)-3-(4-{[2-(2-ethyl-pyrazolo[1,5-*a*]pyridin-3-yl)-ethylamino]-methyl}-phenyl)-N-hydroxy-acrylamide (**25j**). (E)-3-(4-{[2-(2-ethyl-pyrazolo[1,5-*a*]pyridin-3-yl)-ethylamino]-methyl}-phenyl)-acrylic acid methyl ester (1.0 g, 99% yield) was prepared according to general procedure method A from **24j** (530 mg, 2.8 mmol). ¹H NMR (400 MHz, CDCl₃) δ 8.33 (dt, *J* = 7.0, 1.2 Hz, 1 H), 7.51 (d, *J* = 15.9 Hz, 1 H), 7.48–7.39 (m, 5 H), 7.07–7.03 (m, 1 H), 6.69–6.64 (m, 1 H), 6.31 (d, *J* = 15.9 Hz, 1 H), 3.82 (s, 3 H), 3.71 (s, 2 H), 3.45 (t, *J* = 6.4 Hz, 2 H), 2.92 (t, *J* = 7.0 Hz, 2 H), 2.75 (q, *J* = 7.7 Hz, 2 H), 1.28 (t, *J* = 7.7 Hz, 3 H). MS *m/z* 363.9 (MH⁺).

The title compound (47 mg, 47% yield) was prepared according to general procedure method B from (E)-3-(4-{[2-(2-ethyl-pyrazolo[1,5-*a*]pyridin-3-yl)-ethylamino]-methyl}-phenyl)-acrylic acid methyl ester (100 mg, 0.27 mmol). ¹H NMR (400 MHz, CD₃OD) δ 8.43 (d, *J* = 7.0, 1 H), 7.68 (d, *J* = 8.1 Hz, 2 H), 7.63–7.57 (m, 4 H), 7.23 (dd, *J* = 8.7, 6.8 Hz, 1 H), 6.85 (td, *J* = 6.8, 1.0 Hz, 1 H), 6.56 (d, *J* = 16.0 Hz, 1 H), 4.31 (s, 2 H), 3.25–3.16 (m, 4 H), 2.85 (q, *J* = 7.7 Hz, 2 H), 1.34 (t, *J* = 7.6 Hz, 3 H). ¹³C NMR (400 MHz, CD₃OD) δ 165.94, 156.47, 140.82, 140.48, 134.16, 131.7, 129.5, 129.12, 125.11, 119.94, 117.07, 113.08, 103.05, 51.97, 49.75, 20.88, 20.63, 14.57. HRMS C₁₂H₂₅N₄O₂ (MH⁺). calcd 365.1978, found 365.1985.

(E)-N-Hydroxy-3-(4-{[2-(2-phenyl-pyrazolo[1,5-*a*]pyridin-3-yl)-ethylamino]-methyl}-phenyl)-acrylamide (**25k**). (E)-3-(4-{[2-(2-phenyl-pyrazolo[1,5-*a*]pyridin-3-yl)-ethylamino]-methyl}-phenyl)-acrylic acid methyl ester (640 mg, 53% yield) was prepared according to general procedure method A from **24k** (700 mg, 3.0 mmol). ¹H NMR (400 MHz, CDCl₃) δ 8.44 (d, *J* = 6.9 Hz, 1 H), 7.74–7.70 (m, 3 H), 7.52–7.41 (m, 4 H), 7.38 (d, *J* = 7.6 Hz, 2 H), 7.29 (d, *J* = 7.9 Hz, 2 H), 7.11 (dd, *J* = 8.8, 6.8 Hz, 1 H), 6.76 (ddd, *J* = 7.5, 6.2, 0.7 Hz, 1 H), 6.28 (d, *J* = 16.1 Hz, 1 H), 3.86 (s, 3 H), 3.83 (s, 2 H), 3.09 (t, *J* = 7.9 Hz, 2 H), 2.94 (t, *J* = 7.5 Hz, 2 H). MS *m/z* 412.1 (MH⁺).

The title compound (35 mg, 35% yield) was prepared according to general procedure method B from (E)-3-(4-{[2-(2-phenyl-pyrazolo[1,5-*a*]pyridin-3-yl)-ethylamino]-methyl}-phenyl)-acrylic acid methyl ester (100 mg, 0.24 mmol). ¹H NMR (400 MHz, CD₃OD) δ 8.48

(dt, $J = 7.0$, 1.1 Hz, 1 H), 7.70–7.67 (m, 2 H), 7.62 (dt, $J = 9.2$, 1.2 Hz, 1 H), 7.54–7.43 (m, 6 H), 7.27 (d, $J = 8.0$ Hz, 2 H), 7.21 (ddd, $J = 9.0$, 6.6, 1.2 Hz, 1 H), 6.89 (dt, $J = 9.7$, 3.5 Hz, 1 H), 6.47 (d, $J = 15.8$ Hz, 1 H), 3.74 (s, 2 H), 3.13 (t, $J = 7.8$ Hz, 2 H), 2.78 (t, $J = 7.8$ Hz, 2 H). ^{13}C NMR (400 MHz, CD_3OD) δ 166.35, 153.31, 142.23, 141.45, 141.14, 135.23, 134.58, 131.05, 130.07, 129.78, 129.47, 129.07, 128.92, 124.66, 118.35, 118.03, 113.71, 106.78, 53.54, 49.86, 24.03. MS m/z 412.9 (MH^+). HRMS calcd for $\text{C}_{25}\text{H}_{24}\text{N}_4\text{O}_2$ (M^-) 411.1821, found 411.1830.

(*E*)-*N*-Hydroxy-3-[4-({isopropyl-[2-(2-methyl-pyrazolo[1,5-*a*]pyridin-3-yl)-ethyl]-amino}-methyl)-phenyl]-acrylamide (**25l**). (*E*)-3-[4-({isopropyl-[2-(2-methyl-pyrazolo[1,5-*a*]pyridin-3-yl)-ethyl]-amino}-methyl)-phenyl]-acrylic acid methyl ester (400 mg, 70% yield) was prepared according to same procedure as the intermediate for **25m** below from (*E*)-3-[4-({[2-(2-methyl-pyrazolo[1,5-*a*]pyridin-3-yl)-ethylamino]-methyl}-phenyl)-acrylic acid methyl ester (900 mg, 2.48 mmol). ^1H NMR (400 MHz, CDCl_3) δ 8.27 (dt, $J = 7.0$, 1.2 Hz, 1 H), 7.68 (d, $J = 16.7$ Hz, 1 H), 7.40 (d, $J = 7.5$ Hz, 2 H), 7.30 (d, $J = 8.0$ Hz, 2 H), 7.09 (dt, $J = 8.8$, 1.2 Hz, 1 H), 6.89 (ddd, $J = 8.8$, 6.7, 1.1 Hz, 1 H), 6.56 (td, $J = 6.9$, 1.4 Hz, 1 H), 6.41 (d, $J = 16.0$ Hz, 1 H), 3.81 (s, 3 H), 3.62 (s, 2 H), 3.05 (sept, $J = 6.5$ Hz, 1 H), 2.69 (t, $J = 7.6$ Hz, 2 H), 2.56 (t, $J = 7.9$ Hz, 2 H), 2.32 (s, 3 H), 1.05 (d, $J = 6.3$ Hz, 6 H). MS m/z 391.9 (MH^+).

The title compound (280 mg, 72% yield) was prepared according to method B from (*E*)-3-[4-({isopropyl-[2-(2-methyl-pyrazolo[1,5-*a*]pyridin-3-yl)-ethyl]-amino}-methyl)-phenyl]-acrylic acid methyl ester (390 mg, 0.99 mmol). ^1H NMR (400 MHz, CD_3OD) δ 8.29 (dt, $J = 7.0$, 1.1 Hz, 1 H), 7.48 (d, $J = 16.1$ Hz, 1 H), 7.35 (d, $J = 8.3$ Hz, 2 H), 7.21–7.18 (m, 3 H), 7.00 (ddd, $J = 8.9$, 6.7, 1.0 Hz, 1 H), 6.70 (dt, $J = 9.5$, 3.5 Hz, 1 H), 6.44 (d, $J = 16.0$ Hz, 1 H), 3.60 (s, 2 H), 3.13 (sept, $J = 6.6$ Hz, 1 H), 2.72 (t, $J = 7.1$ Hz, 2 H), 2.61 (t, $J = 7.2$ Hz, 2 H), 2.27 (s, 3 H), 1.11 (d, $J = 6.5$ Hz, 6 H). MS m/z 393.0 (MH^+). HRMS calcd for $\text{C}_{23}\text{H}_{28}\text{N}_4\text{O}_2$ (MH^+) 393.2291, found 39.2289.

(*E*)-3-[4-({[2-(2-Ethyl-pyrazolo[1,5-*a*]pyridin-3-yl)-ethyl]-isopropyl-amino}-methyl)-phenyl]-*N*-hydroxy-acrylamide (**25m**). (*E*)-3-[4-({[2-(2-Ethyl-pyrazolo[1,5-*a*]pyridin-3-yl)-ethylamino]-methyl}-phenyl)-acrylic acid methyl ester (900 mg, 2.48 mmol) was added to a solution of 2-iodo-propane (4.21 g, 24.8 mmol) and triethylamine (3.44 mL, 24.8 mmol) in CH_3CN (20 mL). The mixture was refluxed overnight. The solvent was then removed under vacuum. EtOAc and water were added. The aqueous layer was extracted several times with EtOAc. The combined organic layers were washed with brine, dried over Na_2SO_4 , filtered, and evaporated off. The crude product was purified via flash column chromatography (EtOAc:hexanes, 10:90 to 100:0) to provide (*E*)-3-[4-({[2-(2-ethyl-pyrazolo[1,5-*a*]pyridin-3-yl)-ethyl]-isopropyl-amino}-methyl)-phenyl]-acrylic acid methyl ester as a slightly yellow oil (300 mg, 30% yield). ^1H NMR (400 MHz, CDCl_3) δ 8.30 (dt, $J = 7.0$, 1.2 Hz, 1 H), 7.69 (d, $J = 16.1$ Hz, 1 H), 7.42 (d, $J = 7.9$ Hz, 2 H), 7.34 (d, $J = 8.0$ Hz, 2 H), 7.11 (dt, $J = 8.8$, 1.3 Hz, 1 H), 6.90 (ddd, $J = 8.9$, 6.6, 1.2 Hz, 1 H), 6.57 (ddd, $J = 7.8$, 6.0, 0.7 Hz, 1 H), 6.42 (d, $J = 15.9$ Hz, 1 H), 3.81 (s, 3 H), 3.64 (s, 2 H), 3.06 (sept, $J = 6.6$ Hz, 1 H), 2.72–2.66 (m, 4 H), 2.56 (t, $J = 8.1$ Hz, 2 H), 1.24 (t, $J = 7.6$ Hz, 3 H), 1.07 (d, $J = 6.8$ Hz, 6 H). MS m/z 406.6 (MH^+).

The title compound (160 mg, 54% yield) was prepared according to the general procedure method B from (*E*)-3-[4-({[2-(2-ethyl-pyrazolo[1,5-*a*]pyridin-3-yl)-ethyl]-isopropyl-amino}-methyl)-phenyl]-acrylic acid methyl ester (300 mg, 0.73 mmol). ^1H NMR (400 MHz, CD_3OD) δ 8.30 (d, $J = 6.9$ Hz, 1 H), 7.54 (d, $J = 15.8$ Hz, 1 H), 7.40 (d, $J = 8.3$ Hz, 2 H), 7.26 (d, $J = 7.8$ Hz, 2 H), 7.21 (d, $J = 8.7$ Hz, 1 H), 7.01 (ddd, $J = 8.9$, 6.7, 1.0 Hz, 1 H), 6.70 (dt, $J = 9.5$, 3.5 Hz, 1 H), 6.43 (d, $J = 15.8$ Hz, 1 H), 3.66 (s, 2 H), 3.18 (sept, $J = 6.4$ Hz, 1 H), 2.72 (t, $J = 7.2$ Hz, 2 H), 2.66–2.60 (m, 4 H), 1.19 (t, $J = 7.6$ Hz, 3 H), 1.14 (d, $J = 6.4$ Hz, 6 H). ^{13}C NMR (400 MHz, CD_3OD) δ 166.48, 155.99, 141.52, 140.59, 134.96, 130.65, 128.71, 128.63, 123.98, 117.96, 117.47, 112.45, 107.15, 54.77, 52.10, 51.68, 23.36, 20.64, 18.36, 14.63. MS m/z 407.0 (MH^+). HRMS $\text{C}_{24}\text{H}_{30}\text{N}_4\text{O}_2$ (M^-) calcd 405.2291, found 405.2323

(*E*)-*N*-Hydroxy-3-[4-({isopropyl-[2-(2-phenyl-pyrazolo[1,5-*a*]pyridin-3-yl)-ethyl]-amino}-methyl)-phenyl]-acrylamide (**25n**). (*E*)-3-[4-({isopropyl-[2-(2-phenyl-pyrazolo[1,5-*a*]pyridin-3-yl)-ethyl]-amino}-methyl)-phenyl]-acrylic acid methyl ester (300 mg, 52% yield) was prepared according to same procedure as above from (*E*)-3-[4-({[2-(2-phenyl-pyrazolo[1,5-*a*]pyridin-3-yl)-ethylamino]-methyl}-phenyl)-acrylic acid methyl ester (520 mg, 1.26 mmol). ^1H NMR (400 MHz, CDCl_3) δ 8.39 (dt, $J = 7.1$, 1.1 Hz, 1 H), 7.69 (d, $J = 14.5$ Hz, 1 H), 7.66–7.64 (m, 2 H), 7.42–7.37 (m, 5 H), 7.27 (d, $J = 8.6$ Hz, 2 H), 7.20 (dt, $J = 9.0$, 1.4 Hz, 1 H), 6.96 (ddd, $J = 8.9$, 6.6, 1.1 Hz, 1 H), 6.67 (ddd, $J = 7.5$, 6.3, 0.7 Hz, 1 H), 6.42 (d, $J = 15.8$ Hz, 1 H), 3.82 (s, 3 H), 3.57 (s, 2 H), 2.99 (sept, $J = 5.2$ Hz, 1 H), 2.92 (t, $J = 7.6$ Hz, 2 H), 2.62 (t, $J = 7.8$ Hz, 2 H), 1.00 (d, $J = 6.4$ Hz, 6 H). MS m/z 453.9 (MH^+).

The title compound (270 mg, 92% yield) was prepared according to the general procedure method B from (*E*)-3-[4-({isopropyl-[2-(2-phenyl-pyrazolo[1,5-*a*]pyridin-3-yl)-ethyl]-amino}-methyl)-phenyl]-acrylic acid methyl ester (300 mg, 0.66 mmol). ^1H NMR (400 MHz, CD_3OD) δ 8.41 (dt, $J = 7.0$, 1.1 Hz, 1 H), 7.62 (dt, $J = 6.0$, 2.0 Hz, 2 H), 7.47–7.40 (m, 0 H), 7.34 (d, $J = 8.0$ Hz, 2 H), 7.30 (dt, $J = 8.9$, 1.3 Hz, 1 H), 7.15 (d, $J = 8.1$ Hz, 2 H), 7.08 (ddd, $J = 9.0$, 6.7, 1.0 Hz, 1 H), 6.82 (dt, $J = 9.7$, 3.5 Hz, 1 H), 6.47 (d, $J = 15.8$ Hz, 1 H), 3.53 (s, 2 H), 3.02 (sept, $J = 6.6$ Hz, 1 H), 2.93 (t, $J = 7.2$ Hz, 2 H), 2.60 (t, $J = 7.7$ Hz, 2 H), 1.00 (d, $J = 6.5$ Hz, 6 H). ^{13}C NMR (400 MHz, CD_3OD) δ 166.56, 153.26, 144.31, 141.67, 141.3, 134.79, 130.36, 129.79, 129.67, 129.62, 129.35, 129.30, 128.94, 128.9, 128.51, 128.41, 126.34, 124.18, 118.13, 117.73, 113.46, 108.14, 54.69, 54.43, 51.47, 51.34, 23.83, 18.28. HRMS calcd for $\text{C}_{28}\text{H}_{30}\text{N}_4\text{O}_2$ (MH^+) 455.2447, found 455.2442.

■ ASSOCIATED CONTENT

S Supporting Information. Scatter plot of clogP and hERG radioligand displacement IC_{50} . This material is available free of charge via the Internet at <http://pubs.acs.org>.

■ AUTHOR INFORMATION

Corresponding Author

*Phone: 617-871-7551. Fax: 617-871-4081. E-mail: michael.shultz@novartis.com.

Present Addresses

[†]Department of Chemistry, Massachusetts Institute of Technology, Cambridge, Massachusetts, United States.

[‡]Alkermes, 852 Winter Street, Waltham, Massachusetts 02451, United States.

[§]Memorial Sloan Kettering Cancer Center, New York, New York, United States.

^{||}WuXi AppTec, Shanghai, China.

[⊥]Concert Pharmaceuticals Inc., 99 Hayden Avenue, Lexington Massachusetts, 02421, United States.

■ ABBREVIATIONS USED

CSI, cardiac safety index; fwhm, full width at half-maximum; H1299, human nonsmall cell lung cancer cell line; HCT-116, human colorectal carcinoma cell line; HDAC, histone deacetylase; hERG, human ether-a-go-go related gene product; iCSI, in vitro cardiac safety index; PK, pharmacokinetic; SAHA, suberoylanilide hydroxamic acid; SAR, structure–activity relationships

■ REFERENCES

(1) Wang, H.; Holloway, M. P.; Ma, L.; Cooper, Z. A.; Riolo, M.; Samkari, A.; Elenitoba-Johnson, K. S.; Chin, Y. E.; Altura, R. A.

Acetylation directs survivin nuclear localization to repress STAT3 oncogenic activity. *J. Biol. Chem.* **2010**, *46*, 36129–36137.

(2) Lu, Z.; Scott, I.; Webster, B. R.; Sack, M. N. The emerging characterization of lysine residue deacetylation on the modulation of mitochondrial function and cardiovascular biology. *Circ. Res.* **2009**, *105*, 830–841.

(3) Shandilya, J.; Swaminathan, V.; Gadad, S. S.; Choudhari, R.; Kodaganur, G. S.; Kundu, T. K. Acetylated NPM1 localizes in the nucleoplasm and regulates transcriptional activation of genes implicated in oral cancer manifestation. *Mol. Cell. Biol.* **2009**, *29*, 5115–5127.

(4) Faus, H.; Haendler, B. Androgen receptor acetylation sites differentially regulate gene control. *J. Cell Biochem.* **2008**, *104*, 511–524.

(5) di Bari, M. G.; Ciuffini, L.; Mingardi, M.; Testi, R.; Soddu, S.; Barila, D. c-Abl acetylation by histone acetyltransferases regulates its nuclear-cytoplasmic localization. *EMBO Rep.* **2006**, *7*, 727–733.

(6) Zhao, L. J.; Subramanian, T.; Zhou, Y.; Chinnadurai, G. Acetylation by p300 regulates nuclear localization and function of the transcriptional corepressor CtBP2. *J. Biol. Chem.* **2006**, *281*, 4183–4189.

(7) Gay, F.; Calvo, D.; Lo, M. C.; Ceron, J.; Maduro, M.; Lin, R.; Shi, Y. Acetylation regulates subcellular localization of the Wnt signaling nuclear effector POP-1. *Genes Dev.* **2003**, *17*, 717–722.

(8) Du, Z.; Song, J.; Wang, Y.; Zhao, Y.; Guda, K.; Yang, S.; Kao, H. Y.; Xu, Y.; Willis, J.; Markowitz, S. D.; Sedwick, D.; Ewing, R. M.; Wang, Z. DNMT1 Stability Is Regulated by Proteins Coordinating Deubiquitination and Acetylation-Driven Ubiquitination. *Sci. Signaling* **2010**, *3* (ra80), 1–10.

(9) Kim, S.; Jho, E. H. The protein stability of Axin, a negative regulator of Wnt signaling, is regulated by Smad Ubiquitination Regulatory Factor 2. *J. Biol. Chem.* **2010**, *47*, 36420–36426.

(10) Chen, J. Y.; Wang, M. C.; Hung, W. C. Bcr-Abl induced tyrosine phosphorylation of emil to stabilize skp2 protein via inhibition of ubiquitination in chronic myeloid leukemia cells. *J. Cell Physiol.* **2010**, *226*, 407–413.

(11) Nie, J.; Liu, L.; Wu, M.; Xing, G.; He, S.; Yin, Y.; Tian, C.; He, F.; Zhang, L. HECT ubiquitin ligase Smurf1 targets the tumor suppressor ING2 for ubiquitination and degradation. *FEBS Lett.* **2010**, *584*, 3005–3012.

(12) Patwardhan, P.; Resh, M. D. Myristoylation and membrane binding regulate c-Src stability and kinase activity. *Mol. Cell. Biol.* **2010**, *30*, 4094–4107.

(13) Singh, B. N.; Zhang, G.; Hwa, Y. L.; Li, J.; Dowdy, S. C.; Jiang, S. W. Nonhistone protein acetylation as cancer therapy targets. *Expert. Rev. Anticancer Ther.* **2010**, *10*, 935–954.

(14) Mann, B. S.; Johnson, J. R.; Cohen, M. H.; Justice, R.; Pazdur, R. FDA approval summary: vorinostat for treatment of advanced primary cutaneous T-cell lymphoma. *Oncologist* **2007**, *12*, 1247–1252.

(15) Vandermolen, K. M.; McCulloch, W.; Pearce, C. J.; Oberlies, N. H. Romidepsin (Istodax, NSC 630176, FR901228, FK228, depsipeptide): a natural product recently approved for cutaneous T-cell lymphoma. *J. Antibiot. (Tokyo)* **2011**, (Epub ahead of print) doi: 10.1038/ja.2011.35

(16) Thomas, E. A.; Coppola, G.; Desplats, P. A.; Tang, B.; Soragni, E.; Burnett, R.; Gao, F.; Fitzgerald, K. M.; Borok, J. F.; Herman, D.; Geschwind, D. H.; Gottesfeld, J. M. The HDAC inhibitor 4b ameliorates the disease phenotype and transcriptional abnormalities in Huntington's disease transgenic mice. *Proc. Natl. Acad. Sci. U.S.A.* **2008**, *105*, 15564–15569.

(17) Gray, S. G.; Dangond, F. Rationale for the use of histone deacetylase inhibitors as a dual therapeutic modality in multiple sclerosis. *Epigenetics* **2006**, *1*, 67–75.

(18) Minamiyama, M.; Katsuno, M.; Adachi, H.; Waza, M.; Sang, C.; Kobayashi, Y.; Tanaka, F.; Doyu, M.; Inukai, A.; Sobue, G. Sodium butyrate ameliorates phenotypic expression in a transgenic mouse model of spinal and bulbar muscular atrophy. *Hum. Mol. Genet.* **2004**, *13*, 1183–1192.

(19) Pang, M.; Zhuang, S. Histone deacetylase: a potential therapeutic target for fibrotic disorders. *J. Pharmacol. Exp. Ther.* **2010**, *335*, 266–272.

(20) Colussi, C.; Illi, B.; Rosati, J.; Spallotta, F.; Farsetti, A.; Grasselli, A.; Mai, A.; Capogrossi, M. C.; Gaetano, C. Histone deacetylase inhibitors: keeping momentum for neuromuscular and cardiovascular diseases treatment. *Pharmacol. Res.* **2010**, *62*, 3–10.

(21) Cho, Y. K.; Eom, G. H.; Kee, H. J.; Kim, H. S.; Choi, W. Y.; Nam, K. I.; Ma, J. S.; Kook, H. Sodium valproate, a histone deacetylase inhibitor, but not captopril, prevents right ventricular hypertrophy in rats. *Circ. J.* **2010**, *74*, 760–770.

(22) Kee, H. J.; Sohn, I. S.; Nam, K. I.; Park, J. E.; Qian, Y. R.; Yin, Z.; Ahn, Y.; Jeong, M. H.; Bang, Y. J.; Kim, N.; Kim, J. K.; Kim, K. K.; Epstein, J. A.; Kook, H. Inhibition of histone deacetylation blocks cardiac hypertrophy induced by angiotensin II infusion and aortic banding. *Circulation* **2006**, *113*, 51–59.

(23) Meinke, P. T.; Liberator, P. Histone deacetylase: a target for antiproliferative and antiprotozoal agents. *Curr. Med. Chem.* **2001**, *8*, 211–235.

(24) Kavanaugh, S. M.; White, L. A.; Kolesar, J. M. Vorinostat: a novel therapy for the treatment of cutaneous T-cell lymphoma. *Am. J. Health-Syst. Pharm.* **2010**, *67*, 793–797.

(25) Gimsing, P. Belinostat: a new broad acting antineoplastic histone deacetylase inhibitor. *Expert. Opin. Invest. Drugs* **2009**, *18*, 501–508.

(26) Atadja, P.; Hsu, M.; Kwon, P.; Trogani, N.; Bhalla, K.; Remiszewski, S. Molecular and cellular basis for the anti-proliferative effects of the HDAC inhibitor LAQ824. *Novartis Found. Symp.* **2004**, *259*, 249–266.

(27) Yong, W. P.; Goh, B. C.; Soo, R. A.; Toh, H. C.; Ethirajulu, K.; Wood, J.; Novotny-Diermayr, V.; Lee, S. C.; Yeo, W. L.; Chan, D.; Lim, D.; Seah, E.; Lim, R.; Zhu, J. Phase I and pharmacodynamic study of an orally administered novel inhibitor of histone deacetylases, SB939, in patients with refractory solid malignancies. *Ann. Oncol.* **2011**, (advance access) doi: 10.1093/annonc/mdq784.

(28) Bumber, Y.; Younes, A.; Garcia-Manero, G. Mocetinostat (MGCD0103): a review of an isotype-specific histone deacetylase inhibitor. *Expert. Opin. Invest. Drugs* **2011**, *20*, 823–829.

(29) Hess-Stumpp, H.; Bracker, T. U.; Henderson, D.; Politz, O. MS-275, a potent orally available inhibitor of histone deacetylases—the development of an anticancer agent. *Int. J. Biochem. Cell Biol.* **2007**, *39*, 1388–1405.

(30) Piekarz, R. L.; Frye, R.; Prince, H. M.; Kirschbaum, M. H.; Zain, J.; Allen, S. L.; Jaffe, E. S.; Ling, A.; Turner, M.; Peer, C. J.; Figg, W. D.; Steinberg, S. M.; Smith, S.; Joske, D.; Lewis, I.; Hutchins, L.; Craig, M.; Fojo, A. T.; Wright, J. J.; Bates, S. E. Phase II trial of romidepsin in patients with peripheral T-cell lymphoma. *Blood* **2011**, *117*, 5827–5834.

(31) Campas-Moya, C. Romidepsin for the treatment of cutaneous T-cell lymphoma. *Drugs Today* **2009**, *45*, 787–795.

(32) Kouraklis, G.; Theocharis, S. Histone deacetylase inhibitors and anticancer therapy. *Curr. Med. Chem. Anticancer Agents* **2002**, *2*, 477–484.

(33) Marks, P. A.; Richon, V. M.; Kelly, W. K.; Chiao, J. H.; Miller, T. Histone deacetylase inhibitors: development as cancer therapy. *Novartis Found. Symp.* **2004**, *259*, 269–281.

(34) Kouraklis, G.; Theocharis, S. Histone deacetylase inhibitors: a novel target of anticancer therapy (review). *Oncol. Rep.* **2006**, *15*, 489–494.

(35) Mai, A.; Massa, S.; Rotili, D.; Cerbara, I.; Valente, S.; Pezzi, R.; Simeoni, S.; Ragno, R. Histone deacetylation in epigenetics: an attractive target for anticancer therapy. *Med. Res. Rev.* **2005**, *25*, 261–309.

(36) Federico, M.; Bagella, L. Histone deacetylase inhibitors in the treatment of hematological malignancies and solid tumors. *J. Biomed. Biotechnol.* **2011**, *2011*, 475641–475652.

(37) Quintas-Cardama, A.; Santos, F. P.; Garcia-Manero, G. Histone deacetylase inhibitors for the treatment of myelodysplastic syndrome and acute myeloid leukemia. *Leukemia* **2011**, *25*, 226–235.

(38) Carafa, V.; Nebbioso, A.; Altucci, L. Histone deacetylase inhibitors: recent insights from basic to clinical knowledge and patenting of anti-cancer actions. *Recent Pat. Anticancer Drug Discovery* **2011**, *6*, 131–145.

- (39) Jain, N.; Odenike, O. Emerging role of the histone deacetylase inhibitor romidepsin in hematologic malignancies. *Expert Opin. Pharmacother.* **2010**, *11*, 3073–3084.
- (40) Marks, P. A. The clinical development of histone deacetylase inhibitors as targeted anticancer drugs. *Expert Opin. Invest. Drugs* **2010**, *19*, 1049–1066.
- (41) Marsoni, S.; Damia, G.; Camboni, G. A work in progress: the clinical development of histone deacetylase inhibitors. *Epigenetics* **2008**, *3*, 164–171.
- (42) Bruserud, O.; Stapnes, C.; Ersvaer, E.; Gjertsen, B. T.; Rynningen, A. Histone deacetylase inhibitors in cancer treatment: a review of the clinical toxicity and the modulation of gene expression in cancer cell. *Curr. Pharm. Biotechnol.* **2007**, *8*, 388–400.
- (43) Rambaldi, A.; Dellacasa, C. M.; Finazzi, G.; Carobbio, A.; Ferrari, M. L.; Guglielmelli, P.; Gattoni, E.; Salmoiraghi, S.; Finazzi, M. C.; Di, T. S.; D'Urzo, C.; Vannucchi, A. M.; Barosi, G.; Barbui, T. A pilot study of the histone-deacetylase inhibitor Givinostat in patients with JAK2V617F positive chronic myeloproliferative neoplasms. *Br. J. Haematol.* **2010**, *150*, 446–455.
- (44) Molife, R.; Fong, P.; Scurr, M.; Judson, I.; Kaye, S.; de Bono, J. HDAC inhibitors and cardiac safety. *Clin. Cancer Res.* **2007**, *13*, 1068–1069.
- (45) Strevel, E. L.; Ing, D. J.; Siu, L. L. Molecularly targeted oncology therapeutics and prolongation of the QT interval. *J. Clin. Oncol.* **2007**, *25*, 3362–3371.
- (46) Subramanian, S.; Bates, S.; Wright, J.; Espinoza-Delgado, I.; Piekarz, R. Clinical Toxicities of Histone Deacetylase Inhibitors. *Pharmaceuticals* **2010**, *3*, 2751–2767.
- (47) Khan, N.; Jeffers, M.; Kumar, S.; Hackett, C.; Boldog, F.; Khramtsov, N.; Qian, X.; Mills, E.; Berghs, S. C.; Carey, N.; Finn, P. W.; Collins, L. S.; Tumber, A.; Ritchie, J. W.; Jensen, P. B.; Lichenstein, H. S.; Sehested, M. Determination of the class and isoform selectivity of small-molecule histone deacetylase inhibitors. *Biochem. J.* **2008**, *409*, 581–589.
- (48) Beckers, T.; Burkhardt, C.; Wieland, H.; Gimmnich, P.; Ciossek, T.; Maier, T.; Sanders, K. Distinct pharmacological properties of second generation HDAC inhibitors with the benzamide or hydroxamate head group. *Int. J. Cancer* **2007**, *121*, 1138–1148.
- (49) Remiszewski, S. W. The discovery of NVP-LAQ824: from concept to clinic. *Curr. Med. Chem.* **2003**, *10*, 2393–2402.
- (50) Catley, L.; Weisberg, E.; Tai, Y. T.; Atadja, P.; Remiszewski, S.; Hideshima, T.; Mitsiades, N.; Shringarpure, R.; LeBlanc, R.; Chauhan, D.; Munshi, N. C.; Schlossman, R.; Richardson, P.; Griffin, J.; Anderson, K. C. NVP-LAQ824 is a potent novel histone deacetylase inhibitor with significant activity against multiple myeloma. *Blood* **2003**, *102*, 2615–2622.
- (51) Cho, Y. S.; Whitehead, L.; Li, J.; Chen, C. H.; Jiang, L.; Vogtle, M.; Francotte, E.; Richert, P.; Wagner, T.; Traebert, M.; Lu, Q.; Cao, X.; Dumotier, B.; Fejzo, J.; Rajan, S.; Wang, P.; Yan-Neale, Y.; Shao, W.; Atadja, P.; Shultz, M. Conformational refinement of hydroxamate-based histone deacetylase inhibitors and exploration of 3-piperidin-3-ylindole analogues of dacinostat (LAQ824). *J. Med. Chem.* **2010**, *53*, 2952–2963.
- (52) Remiszewski, S. W.; Sambucetti, L. C.; Bair, K. W.; Bontempo, J.; Cesarz, D.; Chandramouli, N.; Chen, R.; Cheung, M.; Cornell-Kennon, S.; Dean, K.; Diamantidis, G.; France, D.; Green, M. A.; Howell, K. L.; Kashi, R.; Kwon, P.; Lassota, P.; Martin, M. S.; Mou, Y.; Perez, L. B.; Sharma, S.; Smith, T.; Sorensen, E.; Taplin, F.; Trogani, N.; Versace, R.; Walker, H.; Weltchek-Engler, S.; Wood, A.; Wu, A.; Atadja, P. N-Hydroxy-3-phenyl-2-propenamides as novel inhibitors of human histone deacetylase with in vivo antitumor activity: discovery of (2E)-N-hydroxy-3-[4-[(2-hydroxyethyl)[2-(1H-indol-3-yl)ethyl]-amino]methyl]phenyl]-2-propenamide (NVP-LAQ824). *J. Med. Chem.* **2003**, *46*, 4609–4624.
- (53) Tamargo, J. Drug-induced torsade de pointes: from molecular biology to bedside. *Jpn. J. Pharmacol.* **2000**, *83*, 1–19.
- (54) Witchel, H. J.; Hancox, J. C. Familial and acquired long qt syndrome and the cardiac rapid delayed rectifier potassium current. *Clin. Exp. Pharmacol. Physiol.* **2000**, *27*, 753–766.
- (55) Recanatini, M.; Poluzzi, E.; Masetti, M.; Cavalli, A.; De, P. F. QT prolongation through hERG K(+) channel blockade: current knowledge and strategies for the early prediction during drug development. *Med. Res. Rev.* **2005**, *25*, 133–166.
- (56) Lagrutta, A. A.; Trepakova, E. S.; Salata, J. J. The hERG channel and risk of drug-acquired cardiac arrhythmia: an overview. *Curr. Top. Med. Chem.* **2008**, *8*, 1102–1112.
- (57) Redfern, W. S.; Carlsson, L.; Davis, A. S.; Lynch, W. G.; MacKenzie, I.; Palethorpe, S.; Siegl, P. K.; Strang, I.; Sullivan, A. T.; Wallis, R.; Camm, A. J.; Hammond, T. G. Relationships between preclinical cardiac electrophysiology, clinical QT interval prolongation and torsade de pointes for a broad range of drugs: evidence for a provisional safety margin in drug development. *Cardiovasc. Res.* **2003**, *58*, 32–45.
- (58) Kerr, J. S.; Galloway, S.; Lagrutta, A.; Armstrong, M.; Miller, T.; Richon, V. M.; Andrews, P. A. Nonclinical safety assessment of the histone deacetylase inhibitor vorinostat. *Int. J. Toxicol.* **2010**, *29*, 3–19.
- (59) Munster, P. N.; Rubin, E. H.; Van, B. S.; Friedman, E.; Patterson, J. K.; Van, D. K.; Li, X.; Comisar, W.; Chodakewitz, J. A.; Wagner, J. A.; Iwamoto, M. A single supratherapeutic dose of vorinostat does not prolong the QTc interval in patients with advanced cancer. *Clin. Cancer Res.* **2009**, *15*, 7077–7084.
- (60) Borchard, U.; Hafner, D. Ion channels and arrhythmias. *Z. Kardiol.* **2000**, *89* (Suppl 3), 6–12.
- (61) Szantay, Cs.; Szabo, L.; Kalas, G. A New Route to Tryptamines. *Synthesis* **1974**, *5*, 354–356.
- (62) Lee, N.; Authier, S.; Pugsley, M. K.; Curtis, M. J. The continuing evolution of torsades de pointes liability testing methods: is there an end in sight? *Toxicol. Appl. Pharmacol.* **2010**, *243*, 146–153.
- (63) Pugsley, M. K.; Hancox, J. C.; Curtis, M. J. Perception of validity of clinical and preclinical methods for assessment of torsades de pointes liability. *Pharmacol. Ther.* **2008**, *119*, 115–117.
- (64) Jones, K. A.; Garbati, N.; Zhang, H.; Large, C. H. Automated patch clamping using the QPatch. *Methods Mol. Biol.* **2009**, *565*, 209–223.
- (65) Kutchinsky, J.; Friis, S.; Asmild, M.; Taborsky, R.; Pedersen, S.; Vestergaard, R. K.; Jacobsen, R. B.; Krzykowski, K.; Schroder, R. L.; Ljungstrom, T.; Helix, N.; Sorensen, C. B.; Bech, M.; Willumsen, N. J. Characterization of potassium channel modulators with QPatch automated patch-clamp technology: system characteristics and performance. *Assay Drug Dev. Technol.* **2003**, *1*, 685–693.
- (66) Tagliatela, M.; Castaldo, P.; Pannaccione, A.; Giorgio, G.; Genovese, A.; Marone, G.; Annunziato, L. Cardiac ion channels and antihistamines: possible mechanisms of cardiotoxicity. *Clin. Exp. Allergy* **1999**, *29* (Suppl 3), 182–189.
- (67) Farid, R.; Day, T.; Friesner, R. A.; Pearlstein, R. A. New insights about HERG blockade obtained from protein modeling, potential energy mapping, and docking studies. *Bioorg. Med. Chem.* **2006**, *14*, 3160–3173.
- (68) Flipo, M.; Charton, J.; Hocine, A.; Dassonneville, S.; Deprez, B.; Deprez-Poulain, R. Hydroxamates: relationships between structure and plasma stability. *J. Med. Chem.* **2009**, *52*, 6790–6802.
- (69) Ihara, M.; Noguchi, K.; Fukumoto, K.; Kametani, T. Conversion of indoles into quinolines through the n-1-c-2 fission by singlet-oxygen as a model experiment of biomimetic synthesis of quinine alkaloids. *Tetrahedron* **1985**, *41*, 2109–2114.
- (70) Szantay, C.; Szabo, L.; Kalas, G. *Synthesis* **1974**, 354–356